Description, Modeling and Simulation Results

of a Test System for Voltage Stability Analysis

Version 6. November 2013

Thierry VAN CUTSEM Lampros PAPANGELIS

University of Liège, Belgium

Contents

1 System overview

The proposed system is a variant of the so-called Nordic32 test system, proposed by K. Walve[1] and detailed in [1]. As indicated in this reference, the system is fictitious but similar to the Swedish and Nordic system (at the time of setting up this test system).

The one-line diagram is shown in Fig. 1.

This system consists of four areas:

- "North" with hydro generation and some load
- "Central" with much load and thermal power generation
- "Equiv" connected to the "North", it includes a very simple equivalent of an external system
- "South" with thermal generation, rather loosely connected to the rest of the system.

The system has rather long transmission lines of 400-kV nominal voltage. Figure 2 shows the structure of the 400-kV backbone, rendering the geographic locations of the stations. Five lines are equipped with series compensation; the percentage of compensation is shown in the figure. The model also includes a representation of some regional systems operating at 220 and 130 kV, respectively (see Fig. 1).

Table 1 gives the active power load and generation in each area and for the whole system.

Table 1: Active power load and generation

area	generated power (MW)	consumed power (MW)
North	4628.5	1180.0
Central	2850.0	6190.0
South	1590.0	1390.0
Equiv	2437.4	2300.0
total	11505.9	11060.0

The nominal frequency is 50 Hz. Frequency is controlled through the speed governors of the hydro generators in the "North" and "Equiv" areas only (see Fig. 1). g20 is an equivalent generator, with a large participation in primary frequency control. The thermal units of the Central and South areas do not participate in this control.

The system is heavily loaded with large transfers essentially from North to Central areas. Secure system operation is limited by transient (angle) and long-term voltage instability. The contingencies likely to yield voltage instability are:

- the tripping of a line in the North-Central corridor, forcing the North-Central power to flow over the remaining lines;

[1] at that time with Svenska Kraftn´et, Sweden

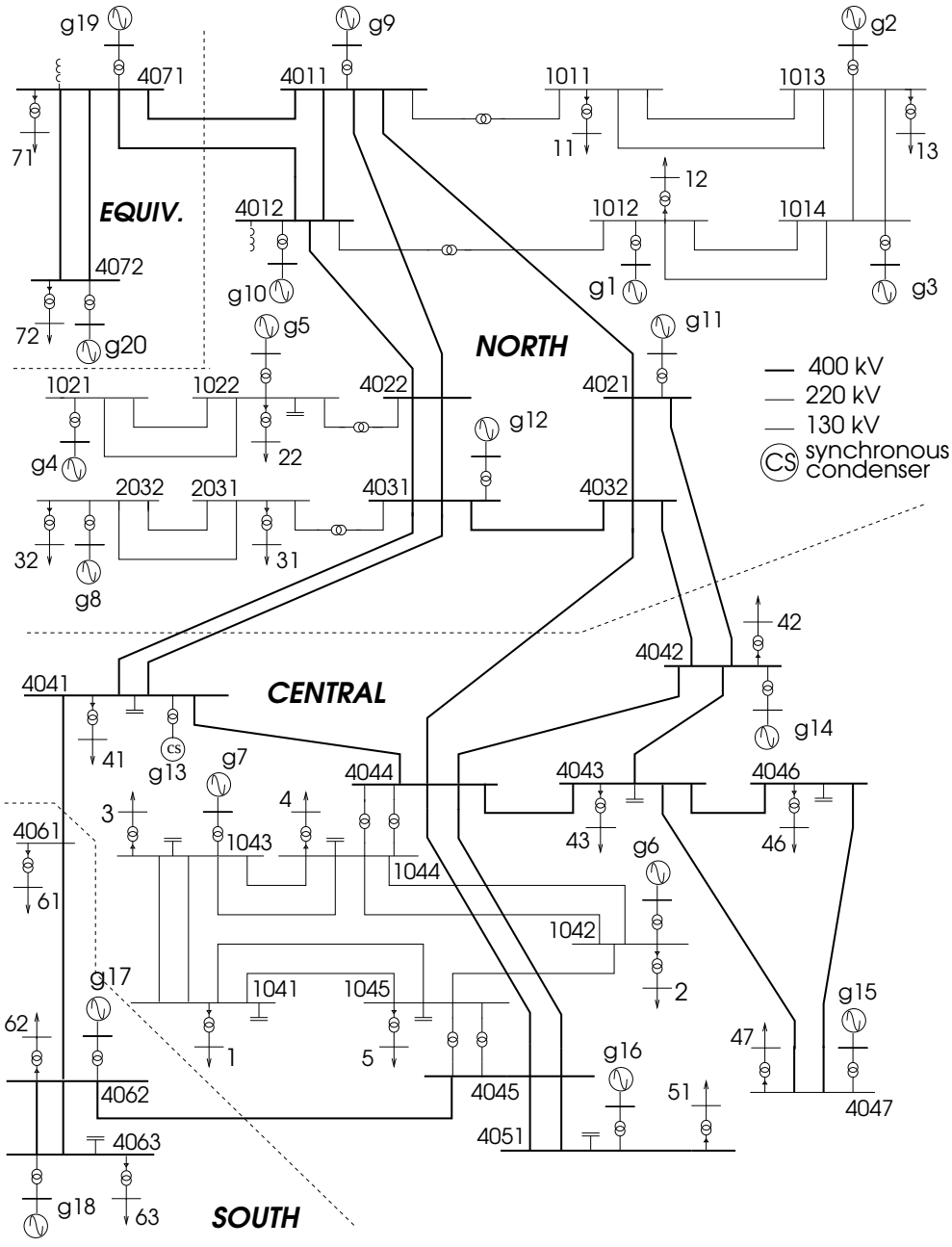

Figure 1: One-line diagram of the test system

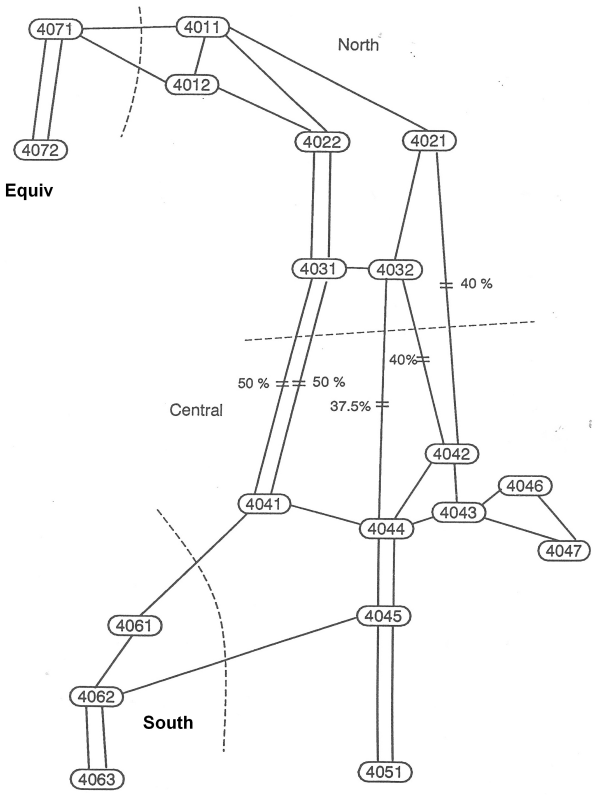

Figure 2: Structure of the 400-kV system

- the outage of a generator located in the Central area, compensated (through speed governors) by the Northern hydro generators, thereby causing an additional power transfer over the North-Central corridor.

The maximum power that can be delivered to the Central loads is strongly influenced by the reactive power capabilities of the Central and some of the Northern generators. Their reactive power limits are enforced by OverExcitation Limiters (OELs). On the other hand, Load Tap Changers (LTCs) aim at restoring distribution voltages and hence load powers. If, after a disturbance (such as a generator or a line outage), the maximum power that can be delivered by the combined generation and transmission system is smaller than what the LTCs attempt to restore, voltage instability results. The latter is of the long-term type. It is driven by OELs and LTCs and takes place in one to two minutes after the initiating event. A similar mechanism takes place in case of a demand increase.

2 Models and data

The model involves 20 generator, 32 transmission and 22 distribution buses, for a total of 74 buses. It includes 102 branches, among which 22 distribution and 20 step-up transformers.

2.1 Network data

The line parameters are given in Table 2 and 3, respectively. The nominal apparent power S_{nom} is given for information. For series-compensated lines (see Fig. 2), the reactance X accounts for the series capacitor (i.e. the series reactance has been decreased accordingly).

Table 2: Transmission line data

line name	from bus	to bus	R (Ω)	X (Ω)	$\omega C/2$ (μS)	S_{nom} (MVA)
1011-1013	1011	1013	1.69	11.83	40.841	350.
1011-1013b	1011	1013	1.69	11.83	40.841	350.
1012-1014	1012	1014	2.37	15.21	53.407	350.
1012-1014b	1012	1014	2.37	15.21	53.407	350.
1013-1014	1013	1014	1.18	8.450	29.845	350.
1013-1014b	1013	1014	1.18	8.450	29.845	350.
1021-1022	1021	1022	5.07	33.80	89.535	350.
1021-1022b	1021	1022	5.07	33.80	89.535	350.
1041-1043	1041	1043	1.69	10.14	36.128	350.
1041-1043b	1041	1043	1.69	10.14	36.128	350.
1041-1045	1041	1045	2.53	20.28	73.827	350.
1041-1045b	1041	1045	2.53	20.28	73.827	350.
1042-1044	1042	1044	6.42	47.32	177.50	350.
1042-1044b	1042	1044	6.42	47.32	177.50	350.
1042-1045	1042	1045	8.45	50.70	177.50	350.
1043-1044	1043	1044	1.69	13.52	47.124	350.
1043-1044b	1043	1044	1.69	13.52	47.124	350.
2031-2032	2031	2032	5.81	43.56	15.708	500.
2031-2032b	2031	2032	5.81	43.56	15.708	500.
4011-4012	4011	4012	1.60	12.80	62.832	1400.
4011-4021	4011	4021	9.60	96.00	562.34	1400.
4011-4022	4011	4022	6.40	64.00	375.42	1400.
4011-4071	4011	4071	8.00	72.00	438.25	1400.
4012-4022	4012	4022	6.40	56.00	328.30	1400.
4012-4071	4012	4071	8.00	80.00	468.10	1400.
4021-4032	4021	4032	6.40	64.00	375.42	1400.

Table 3: Transmission line data (cont'd)

line name	from bus	to bus	R (Ω)	X (Ω)	$\omega C/2$ (μS)	S_{nom} (MVA)
4021-4042	4021	4042	16.0	96.00	937.77	1400.
4022-4031	4022	4031	6.40	64.00	375.42	1400.
4022-4031b	4022	4031	6.40	64.00	375.42	1400.
4031-4032	4031	4032	1.60	16.00	94.248	1400.
4031-4041	4031	4041	9.60	64.00	749.27	1400.
4031-4041b	4031	4041	9.60	64.00	749.27	1400.
4032-4042	4032	4042	16.0	64.00	625.18	1400.
4032-4044	4032	4044	9.60	80.00	749.27	1400.
4041-4044	4041	4044	4.80	48.00	281.17	1400.
4041-4061	4041	4061	9.60	72.00	406.84	1400.
4042-4043	4042	4043	3.20	24.00	155.51	1400.
4042-4044	4042	4044	3.20	32.00	186.93	1400.
4043-4044	4043	4044	1.60	16.00	94.248	1400.
4043-4046	4043	4046	1.60	16.00	94.248	1400.
4043-4047	4043	4047	3.20	32.00	186.93	1400.
4044-4045	4044	4045	3.20	32.00	186.93	1400.
4044-4045b	4044	4045	3.20	32.00	186.93	1400.
4045-4051	4045	4051	6.40	64.00	375.42	1400.
4045-4051b	4045	4051	6.40	64.00	375.42	1400.
4045-4062	4045	4062	17.6	128.00	749.27	1400.
4046-4047	4046	4047	1.60	24.00	155.51	1400.
4061-4062	4061	4062	3.20	32.00	186.93	1400.
4062-4063	4062	4063	4.80	48.00	281.17	1400.
4062-4063b	4062	4063	4.80	48.00	281.17	1400.
4071-4072	4071	4072	4.80	48.00	937.77	1400.
4071-4072b	4071	4072	4.80	48.00	937.77	1400.

The transformer data are given in Tables 4 to 6. The resistance corresponding to copper losses and the magnetizing susceptance are neglected. For the orientation of the transformer, please refer to Fig. 3. X is in per unit on the base (V_{Bfrom}, S_{nom}) where V_{Bfrom} is the network base voltage of the "from" bus and S_{nom} the nominal apparent power of the transformer. n is in pu/pu on the base (V_{Bto}, V_{Bfrom}), where V_{Bto} is the network base voltage of the "to" bus.

The step-up transformers of all generators and the step-down transformers of all loads are represented explicitly.

The step-down transformers have their ratios adjusted in the initial power flow calculation so that the distribution bus voltage is 1. pu.

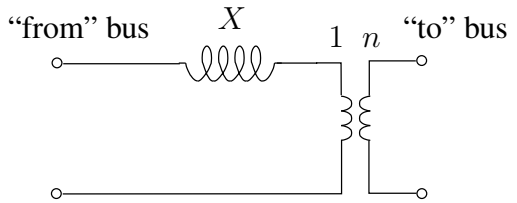

Figure 3: Transformer representation

Table 4: Data of the step-up transformers

transformer name	from bus	to bus	X (pu)	n (pu/pu)	S_{nom} (MVA)
g1	g1	1012	0.15	1.00	800.0
g2	g2	1013	0.15	1.00	600.0
g3	g3	1014	0.15	1.00	700.0
g4	g4	1021	0.15	1.00	600.0
g5	g5	1022	0.15	1.05	250.0
g6	g6	1042	0.15	1.05	400.0
g7	g7	1043	0.15	1.05	200.0
g8	g8	2032	0.15	1.05	850.0
g9	g9	4011	0.15	1.05	1000.0
g10	g10	4012	0.15	1.05	800.0
g11	g11	4021	0.15	1.05	300.0
g12	g12	4031	0.15	1.05	350.0
g13	g13	4041	0.10	1.05	300.0
g14	g14	4042	0.15	1.05	700.0
g15	g15	4047	0.15	1.05	1200.0
g16	g16	4051	0.15	1.05	700.0
g17	g17	4062	0.15	1.05	600.0
g18	g18	4063	0.15	1.05	1200.0
g19	g19	4071	0.15	1.05	500.0
g20	g20	4072	0.15	1.05	4500.0

Table 5: Data of the 400/220 and 400/130 transformers

transformer name	from bus	to bus	X (pu)	n (pu/pu)	S_{nom} (MVA)
1011-4011	1011	4011	0.10	0.95	1250.0
1012-4012	1012	4012	0.10	0.95	1250.0
1022-4022	1022	4022	0.10	0.93	833.3
2031-4031	2031	4031	0.10	1.00	833.3
1044-4044	1044	4044	0.10	1.03	1000.0
1044-4044b	1044	4044	0.10	1.03	1000.0
1045-4045	1045	4045	0.10	1.04	1000.0
1045-4045b	1045	4045	0.10	1.04	1000.0

Table 6: Data of the step-down transformers

transformer name	from bus	to bus	X (pu)	n (pu/pu)	S_{nom} (MVA)
11-1011	11	1011	0.10	1.04	400.0
12-1012	12	1012	0.10	1.05	600.0
13-1013	13	1013	0.10	1.04	200.0
22-1022	22	1022	0.10	1.04	560.0
1-1041	1	1041	0.10	1.00	1200.0
2-1042	2	1042	0.10	1.00	600.0
3-1043	3	1043	0.10	1.01	460.0
4-1044	4	1044	0.10	0.99	1600.0
5-1045	5	1045	0.10	1.00	1400.0
31-2031	31	2031	0.10	1.01	200.0
32-2032	32	2032	0.10	1.06	400.0
41-4041	41	4041	0.10	1.04	1080.0
42-4042	42	4042	0.10	1.03	800.0
43-4043	43	4043	0.10	1.02	1800.0
46-4046	46	4046	0.10	1.02	1400.0
47-4047	47	4047	0.10	1.04	200.0
51-4051	51	4051	0.10	1.05	1600.0
61-4061	61	4061	0.10	1.03	1000.0
62-4062	62	4062	0.10	1.04	600.0
63-4063	63	4063	0.10	1.03	1180.0
71-4071	71	4071	0.10	1.03	600.0
72-4072	72	4072	0.10	1.05	4000.0

The shunt capacitor/inductor data are given in Table 7. Q_{nom} is the reactive power produced by the shunt element under a 1 pu voltage. Negative values relate to inductors.

Table 7: Shunt compensation data

bus	Q_{nom} (Mvar)
1022	50.
1041	250.
1043	200.
1044	200.
1045	200.
4012	-100.
4041	200.
4043	200.
4046	100.
4051	100.
4071	-400.

2.2 Operating point data

Two operating points are considered. The first one, denoted A, is insecure, i.e. the system cannot stand some N-1 contingencies.

The system is made secure by rather simple modifications; this leads to operating point B.

2.2.1 Operating point A

The system operating point is specified in Tables 8 to 10, which provide, for each bus, the consumed active and reactive power, the generated active and reactive power and the initial voltage obtained from a power flow calculation. In this calculation, bus g20 has been taken as slack-bus.

Table 8: Operating point A: data of generator buses

bus	base	consumed power		generated power		initial voltage	
	voltage	active	reactive	active	reactive	magnitude	phase angle
	(kV)	(MW)	(Mvar)	(MW)	(Mvar)	(pu)	(deg)
g1	15.0	0.	0.	600.0	58.3	1.0684	2.59
g2	15.0	0.	0.	300.0	17.2	1.0565	5.12
g3	15.0	0.	0.	550.0	20.9	1.0595	10.27
g4	15.0	0.	0.	400.0	30.4	1.0339	8.03
g5	15.0	0.	0.	200.0	60.1	1.0294	-12.36
g6	15.0	0.	0.	360.0	138.6	1.0084	-59.42
g7	15.0	0.	0.	180.0	60.4	1.0141	-68.95
g8	15.0	0.	0.	750.0	232.6	1.0498	-16.81
g9	15.0	0.	0.	668.5	201.3	0.9988	-1.63
g10	15.0	0.	0.	600.0	255.7	1.0157	0.99
g11	15.0	0.	0.	250.0	60.7	1.0211	-29.04
g12	15.0	0.	0.	310.0	98.3	1.0200	-31.88
g13	15.0	0.	0.	0.0	50.1	1.0170	-54.30
g14	15.0	0.	0.	630.0	295.9	1.0454	-49.90
g15	15.0	0.	0.	1080.0	377.9	1.0455	-52.19
g16	15.0	0.	0.	600.0	222.6	1.0531	-64.10
g17	15.0	0.	0.	530.0	48.7	1.0092	-46.85
g18	15.0	0.	0.	1060.0	293.4	1.0307	-43.32
g19	15.0	0.	0.	300.0	121.2	1.0300	0.03
g20	15.0	0.	0.	2137.4	377.4	1.0185	0.00

Table 9: Operating point A: data of transmission buses

bus	base	consumed power		generated power		initial voltage	
	voltage	active	reactive	active	reactive	magnitude	phase angle
	(kV)	(MW)	(Mvar)	(MW)	(Mvar)	(pu)	(deg)
1011	130.0	0.	0.	0.	0.	1.0618	-6.65
1012	130.0	0.	0.	0.	0.	1.0634	-3.10
1013	130.0	0.	0.	0.	0.	1.0548	1.26
1014	130.0	0.	0.	0.	0.	1.0611	4.26
1021	130.0	0.	0.	0.	0.	1.0311	2.64
1022	130.0	0.	0.	0.	0.	1.0512	-19.05
1041	130.0	0.	0.	0.	0.	1.0124	-81.87
1042	130.0	0.	0.	0.	0.	1.0145	-67.38
1043	130.0	0.	0.	0.	0.	1.0274	-76.77
1044	130.0	0.	0.	0.	0.	1.0066	-67.71
1045	130.0	0.	0.	0.	0.	1.0111	-71.66
2031	220.0	0.	0.	0.	0.	1.0279	-36.66
2032	220.0	0.	0.	0.	0.	1.0695	-23.92
4011	400.0	0.	0.	0.	0.	1.0224	-7.55
4012	400.0	0.	0.	0.	0.	1.0235	-5.54
4021	400.0	0.	0.	0.	0.	1.0488	-36.08
4022	400.0	0.	0.	0.	0.	0.9947	-20.86
4031	400.0	0.	0.	0.	0.	1.0367	-39.46
4032	400.0	0.	0.	0.	0.	1.0487	-44.54
4041	400.0	0.	0.	0.	0.	1.0506	-54.30
4042	400.0	0.	0.	0.	0.	1.0428	-57.37
4043	400.0	0.	0.	0.	0.	1.0370	-63.51
4044	400.0	0.	0.	0.	0.	1.0395	-64.23
4045	400.0	0.	0.	0.	0.	1.0533	-68.88
4046	400.0	0.	0.	0.	0.	1.0357	-64.11
4047	400.0	0.	0.	0.	0.	1.0590	-59.55
4051	400.0	0.	0.	0.	0.	1.0659	-71.01
4061	400.0	0.	0.	0.	0.	1.0387	-57.93
4062	400.0	0.	0.	0.	0.	1.0560	-54.36
4063	400.0	0.	0.	0.	0.	1.0536	-50.68
4071	400.0	0.	0.	0.	0.	1.0484	-4.99
4072	400.0	0.	0.	0.	0.	1.0590	-3.98

Table 10: Operating point A: data of distribution buses

bus	base voltage (kV)	consumed power active (MW)	consumed power reactive (Mvar)	generated power active (MW)	generated power reactive (Mvar)	initial voltage magnitude (pu)	initial voltage phase angle (deg)
1	20.	600.	148.2	0.	0.	0.9988	-84.71
2	20.	330.	71.0	0.	0.	1.0012	-70.49
3	20.	260.	83.8	0.	0.	0.9974	-79.97
4	20.	840.	252.0	0.	0.	0.9996	-70.67
5	20.	720.	190.4	0.	0.	0.9961	-74.59
11	20.	200.	68.8	0.	0.	1.0026	-9.45
12	20.	300.	83.8	0.	0.	0.9975	-5.93
13	20.	100.	34.4	0.	0.	0.9957	-1.58
22	20.	280.	79.9	0.	0.	0.9952	-21.89
31	20.	100.	24.7	0.	0.	1.0042	-39.47
32	20.	200.	39.6	0.	0.	0.9978	-26.77
41	20.	540.	131.4	0.	0.	0.9967	-57.14
42	20.	400.	127.4	0.	0.	0.9952	-60.22
43	20.	900.	254.6	0.	0.	1.0013	-66.33
46	20.	700.	211.8	0.	0.	0.9990	-66.93
47	20.	100.	44.0	0.	0.	0.9950	-62.38
51	20.	800.	258.2	0.	0.	0.9978	-73.84
61	20.	500.	122.5	0.	0.	0.9949	-60.78
62	20.	300.	83.8	0.	0.	1.0002	-57.18
63	20.	590.	264.6	0.	0.	0.9992	-53.49
71	20.	300.	83.8	0.	0.	1.0028	-7.80
72	20.	2000.	396.1	0.	0.	0.9974	-6.83

2.2.2 Operating point B

Operating point B is obtained from operating A by making the following changes.

- In parallel with g16 and its step-up transformer are connected an identical generator - named g16b - and an identical step-up transformer. The additional generator produces the same active power under the same terminal voltage(respectively 600 MW and 1.0531 pu: see Table 8). The additional production of 600 MW is compensated by the slack-bus. The power flow in the North-Central corridor is decreased by almost the same power, which makes the system significantly more robust.
- Still, the system could not stand the loss of either g15 or g18 (producing respectively 1080 and 1060 MW : see Table 8)[2]. Here, the choice is to make the contingencies less severe, by replacing each of these generators by two identical generators with half nominal apparent power (600 instead of 1200 MVA: see Table 11), half nominal turbine power (540 instead of 1080 MW: see same table), and half production (540 instead of 1080 MW for g15, 530 instead of 1060 MW for g18). Each generator is connected to the rest of the system by a step-up transformer with half nominal apparent power (600

[2]indeed, the lost production is compensated by generators in the North and Equiv areas, which increases the flow in the North-Central corridor by the corresponding power

instead of 1200 MVA: see table 4). Both generators have the same terminal voltage as the generator they replace.

Figure 4 compares the input data and some results of power flow calculations at points A and B, respectively.

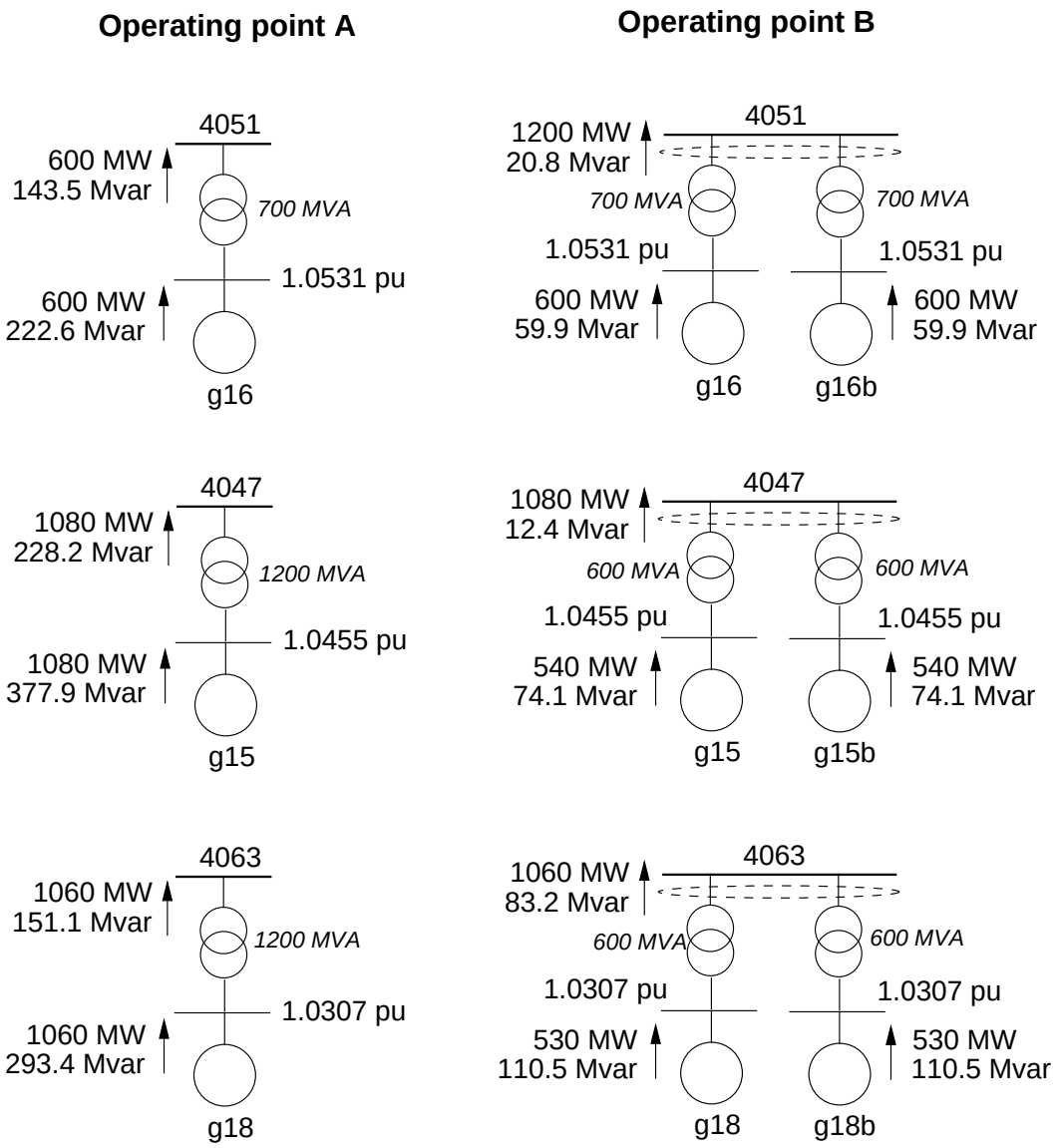

Figure 4: (partial) comparison of operating points A and B

2.3 Synchronous machine data

Synchronous machines are represented by a standard model (e.g. [2]) with three rotor winding for the salient-pole machines of hydro power plants, and four rotor windings for the round-rotor machines of thermal plants. g13 is a synchronous condenser.

The nominal apparent power S_{nom} of each generator together with the nominal active power P_{nom} of its turbine are given in Table 11. As can be seen, the generator power factor, computed as P_{nom}/S_{nom}, is 0.95 for the hydro plants (North and Equiv areas) and 0.90 for the thermal plants (Central and South areas, where most of the load is located).

Table 11: Nominal apparent powers of synchronous machines and nominal active powers of their turbines

gener.	S_{nom} (MVA)	P_{nom} (MW)
g1	800.	760.0
g2	600.	570.0
g3	700.	665.0
g4	600.	570.0
g5	250.	237.5
g6	400.	360.0
g7	200.	180.0
g8	850.	807.5
g9	1000.	950.0
g10	800.	760.0
g11	300.	285.0
g12	350.	332.5
g13	300.	-
g14	700.	630.0
g15	1200.	1080.0
g16	700.	630.0
g17	600.	540.0
g18	1200.	1080.0
g19	500.	475.0
g20	4500.	4275.0

The machine reactances, time constants and inertia coefficients are given in Table 12. The reactances are in pu on the base (V_B, S_{nom}) where V_B is the network base voltage of the machine bus.

Saturation is modelled in all machines. The standard saturation curve relating the no-load armature voltage V_{nl} to the field current i_{fd} is given in Fig. 5. The saturation characteristics is given by:

$$k = \frac{|AC|}{|AB|} = 1 + m(V_{nl})^n$$

The following data apply to all machines:

- for $V_{nl} = 1$ pu, $k = 1.1$ which yields $1.1 = 1 + m$ and hence $m = 0.1$
- for $V_{nl} = 1.2$ pu, $k = 1.3$ which yields $1.3 = 1 + 0.1 \times 1.2^n$ and hence $n = 6.0257$

Table 12: Synchronous machine data

	round rotor	salient pole	salient-pole
	g6, g7, g14, g15, g16, g17, g18	g1, g2, g3, g4, g5, g8, g9, g10, g11, g12, g19, g20	g13
X_d (pu)	2.20	1.10	1.55
X_q (pu)	2.00	0.70	1.00
X'_d (pu)	0.30	0.25	0.30
X'_q (pu)	0.40		
X''_d (pu)	0.20	0.20	0.20
X''_q (pu)	0.20	0.20	0.20
T'_{do} (s)	7.0	5.0	7.0
T'_{qo} (s)	1.5		
T''_{do} (s)	0.05	0.05	0.05
T''_{qo} (s)	0.05	0.10	0.10
H (s)	6.0	3.0	2.0
i_{fd}^{rated} (pu)	2.9160	1.8087	2.8170

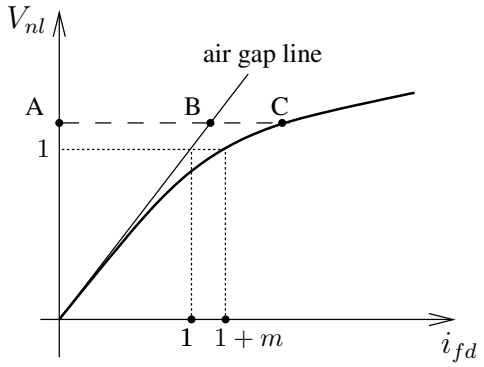

Figure 5: Saturation characteristics

- (unsaturated) leakage reactance $X_\ell = 0.15$ pu in both axes.

The last row in Table 12 provides the generator field currents i_{fd}^{rated} under rated operating conditions, i.e. when the machine operates with:

$$\begin{aligned} V &= 1 \\ P &= P_{nom} \\ S &= S_{nom} \;\Leftrightarrow\; \sqrt{P_{nom}^2 + Q^2} = S_{nom} \;\Leftrightarrow\; Q = \sqrt{S_{nom}^2 - P_{nom}^2} \end{aligned}$$

where P, V and S are in per unit. The i_{fd}^{rated} values are in per unit on a base such that $i_{fd} = 1$ pu when the generator operates at no load with a 1 pu terminal voltage and without saturation (operation on the air gap line). This corresponds to the leftmost point on the abscissa in Fig. 5.

2.4 Exciter, automatic voltage regulator and power system stabilizer model and data

Figure 6 shows the simple model used to represent the exciter, the Automatic Voltage Regulator (AVR) and the Power System Stabilizer (PSS). The same model is used for all generators but with different parameters, as shown in Table 13. v_{fd} is the field voltage, in per unit on a base such that $v_{fd} = 1$ pu when the generator operates at no load with a 1 pu terminal voltage and without saturation (operation on the air gap line). V is the magnitude of the generator terminal voltage, in pu.

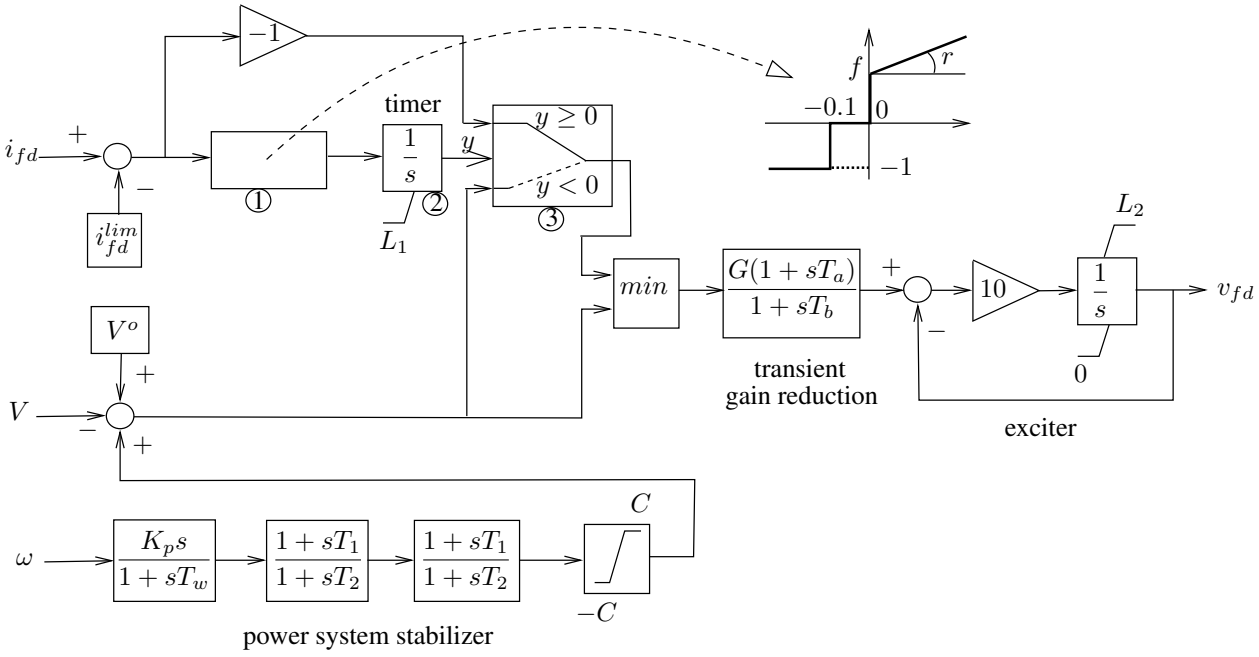

Figure 6: Model of exciter, AVR, PSS and OEL

The exciter is represented by a first-order system with a time constant of 0.1 s and non-windup limits on v_{fd}. The AVR includes a transient gain reduction. The latter has been chosen to limit the overshoot in terminal voltage following a step change in voltage reference when the generator operates in open circuit.

Table 13: Parameters of exciter, AVR, PSS and OEL

generator	i_{fd}^{lim} (pu)	f	r	L_1	G	T_a (s)	T_b (s)	L_2 (pu)	K_p	T_w (s)	T_1 (s)	T_2 (s)	C (pu)
g1, g2, g3	1.8991	0.	1.	-11.	70.	10.	20.0	4.	75.	15.	0.20	0.010	0.1
g4	1.8991	0.	1.	-11.	70.	10.	20.0	4.	150.	15.	0.20	0.010	0.1
g5	1.8991	0.	1.	-11.	70.	10.	20.0	4.	75.	15.	0.20	0.010	0.1
g6	3.0618	1.	0.	-20.	120.	5.	12.5	5.	75.	15.	0.22	0.012	0.1
g7	3.0618	1.	0.	-20.	120.	5.	12.5	5.	75.	15.	0.22	0.012	0.1
g8, g9, g10	1.8991	0.	1.	-11.	70.	10.	20.0	4.	75.	15.	0.20	0.010	0.1
g11	1.8991	1.	0.	-20.	70.	10.	20.0	4.	75.	15.	0.20	0.010	0.1
g12	1.8991	1.	0.	-20.	70.	10.	20.0	4.	75.	15.	0.20	0.010	0.1
g13	2.9579	0.	1.	-17.	50.	4.	20.0	4.	0.				
g14	3.0618	0.	1.	-18.	120.	5.	12.5	5.	75.	15.	0.22	0.012	0.1
g15, g16	3.0618	0.	1.	-18.	120.	5.	12.5	5.	75.	15.	0.22	0.012	0.1
g17, g18	3.0618	0.	1.	-18.	120.	5.	12.5	5.	150.	15.	0.22	0.012	0.1
g19, g20	1.8991	0.	1.	-11.	70.	10.	20.0	4.	0.				

All generators except g13, g19 and g20 are equipped with PSS using the rotor speed ω as input (a zero value for K_p in Table 13 indicates the absence of PSS). ω is in per unit. Each PSS includes a washout filter and two identical lead filters in cascade. The PSS phase compensation was chosen considering the maximum and minimum equivalent Thévenin impedances seen by the machines of each group (units 7 and 18 for the round-rotor, units 4 and 12 for the salient-pole machines). The PSS transfer functions provide damping for oscillation frequencies from 0.2 Hz to more than 1 Hz.

K_p has been set to a higher value for generators g17 and g18, in order these generators to have enough damping after the tripping of line 4061-4062, which leaves them radially connected to the rest of the system. It was also set to a higher value for generator g4, in order to have enough damping after the tripping of line 1021-1022.

No attempt was made to further "optimize" the PSS settings, which is appropriate for a test system.

2.5 Overexcitation limiter model and data

Each machine is equipped with an OverExcitation Limiter (OEL) keeping its field current within limits. Since the focus is on scenarios with sagging voltages and overexcited generators, the model does not include lower excitation limitation. Limits on armature current are not considered either.

The field current limit enforced by the OEL, denoted by i_{fd}^{lim}, is set to 105 % of i_{fd}^{rated}. Thus, if i_{fd} settles to any value below $i_{fd}^{lim} = 1.05\ i_{fd}^{rated}$, the OEL is not activated.

The four smallest generators, namely g6, g7, g11 and g12 have a fixed-time OEL that operates after 20 seconds.

All other machines have an OEL with inverse time characteristics, i.e. the higher the field current, the faster the limitation takes place. This takes advantage of the overload capability of the rotor. For the three types of

generators quoted in Table 12, Figs. 7 to 9 show respectively : the variation of the overload delay with the field current i_{fd} (solid line), four points of the ANSI curve, and the i_{fd}^{lim} value (dashed vertical line). As can be seen, the OEL has been set to react faster than what the ANSI curve allows.

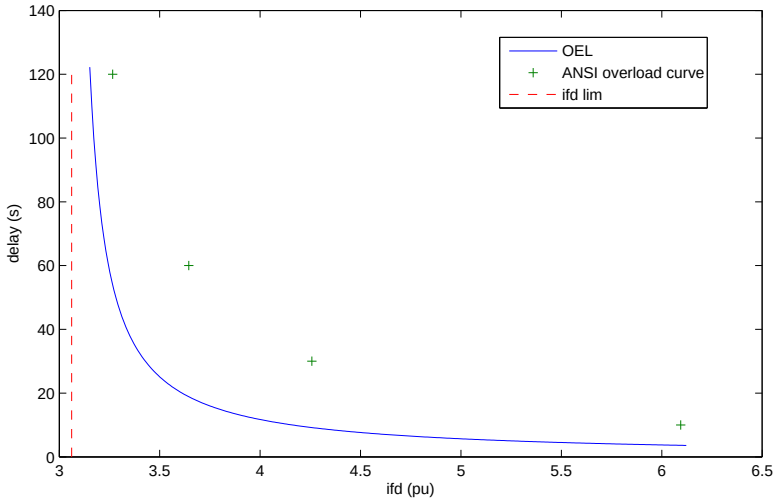

Figure 7: Overexcitation delay: generators g14 - g18

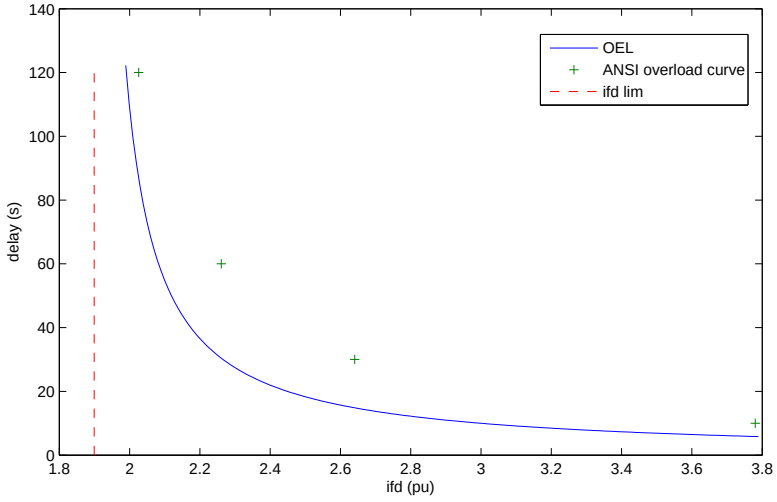

Figure 8: Overexcitation delay: generators g1 - g5, g8 - g10, g19, g20

There is a wide variety of OELs and relatively few standard models [3, 4]. Other models than the one described hereafter can be used provided the correct value i_{fd}^{lim} is enforced after the correct delay.

The OEL model is shown in Fig. 6. It is of the takeover type [4] and applies the so-called "error signal substitution" (the alternative would be the "control signal substitution"). Operation is as follows.

In normal operating conditions i_{fd} is lower than i_{fd}^{lim} and the output of block 1 is -1. This keeps the integrator of block 2 at its lower limit L_1, which is negative. It results that the switch in block 3 remains in the lower

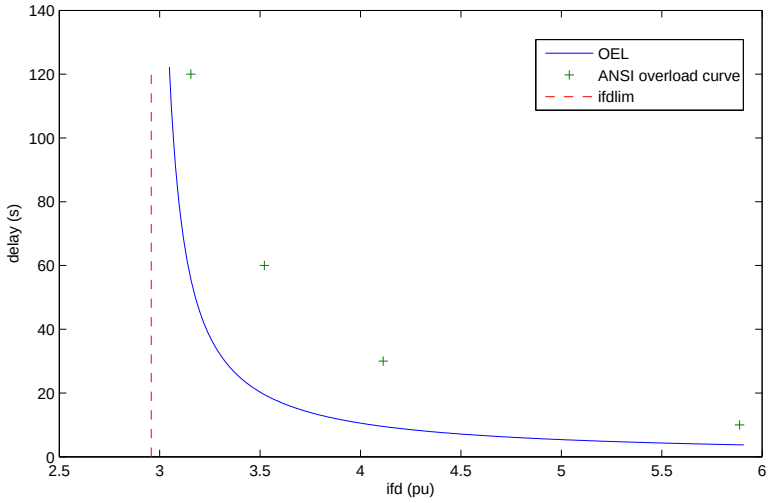

Figure 9: Overexcitation delay: generator g13

position. The minimum gate passes on the $V^o - V$ signal to the AVR.

If i_{fd} becomes larger than i_{fd}^{lim}, the output of block 1 becomes positive, causing the output of block 2 to rise. When it becomes positive, it makes the switch change position, and the negative signal $i_{fd}^{lim} - i_{fd}$ is sent to the minimum gate. The latter selects the signal coming from the OEL, which is thus passed on to the AVR, and the generator changes from voltage to field current control. In steady state, the gain G forces i_{fd} to a value a bit smaller than i_{fd}^{lim}. The difference $i_{fd} - i_{fd}^{lim}$ is expected to lie in the interval $[-0.1\ 0]$. Hence, the output of block 1 is zero (see Fig. 6), which avoids switching back under voltage control.

Block 2 operates as a timer, adding an intentional delay corresponding to the thermal overload capability of the field winding. For generators g6, g7, g11 and g12, $f = 1$ and $r = 0$ (see Table 13). Thus, the switching takes place after a delay that does not depend on the overload $i_{fd} - i_{fd}^{lim}$. The other generators have $f = 0$ and $r = 1$; hence, the larger the overload, the shorter the delay before limiting the field current. This yields the above mentioned inverse-time characteristics.

If the field current has been limited but operating conditions require less excitation, the model automatically resets under voltage control. This is done by the minimum gate choosing the terminal voltage signal.

2.6 Generator capability curves

All the data regarding generator limitations have been given in the previous sections. The steady-state characteristics can be derived in the form of generator capability curves, which are convenient for power flow calculations.

Figures 10 and 11 show the capability curves of respectively the round-rotor and the salient-pole generators,

identified in Columns 2 and 3 of Table 12[3]. In these figures, the powers are in per unit on the MVA machine base; all machines of the same group have the same per unit capability curves.

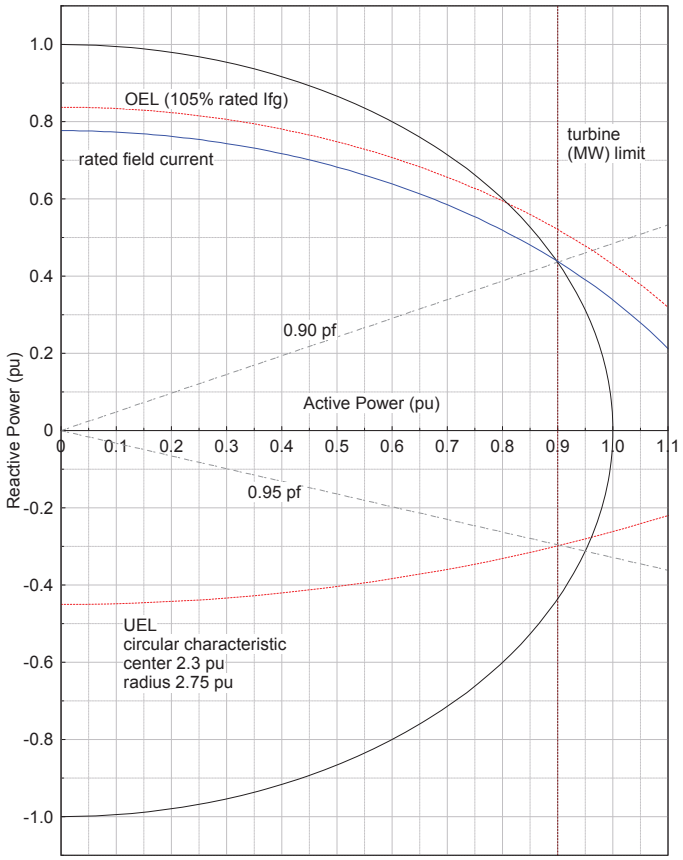

Figure 10: capability curves of round-rotor generators (identified in Table 12)

Note that the curves have been obtained for a 1 pu voltage at the generator bus. They must be adjusted with the generator voltage (base case generator voltages are available in Table 8). Figures 12 and 13 precisely show the field and stator current limits for a terminal voltage equal to 0.95, 1.00 and 1.05 pu, respectively.

From those curves, one can easily obtain the reactive power upper limit Q_{max} of a generator to consider in a power flow calculation. To match the dynamic simulations shown in the next section, only the field current limit is to be considered, since the stator current limit is not enforced.

Example. Consider generator g12 which operates at 1.02 pu voltage and $310/350 = 0.886$ pu of active power. From Figure 13, one obtains $Q_{max} = 0.4$ pu = 0.4×350 = 140 Mvar.

No capability curve is provided for g13, which is a synchronous condenser. The maximum reactive power, corresponding to the rotor current limit is 1.0782 pu (= 323.4 Mvar) at 1 pu voltage, 1.0926 pu (= 327.8 Mvar) at 0.95 pu voltage, and 1.0488 pu (= 314.6 Mvar) at 1.05 pu voltage.

[3]the synchronous condenser at bus g13 is not considered

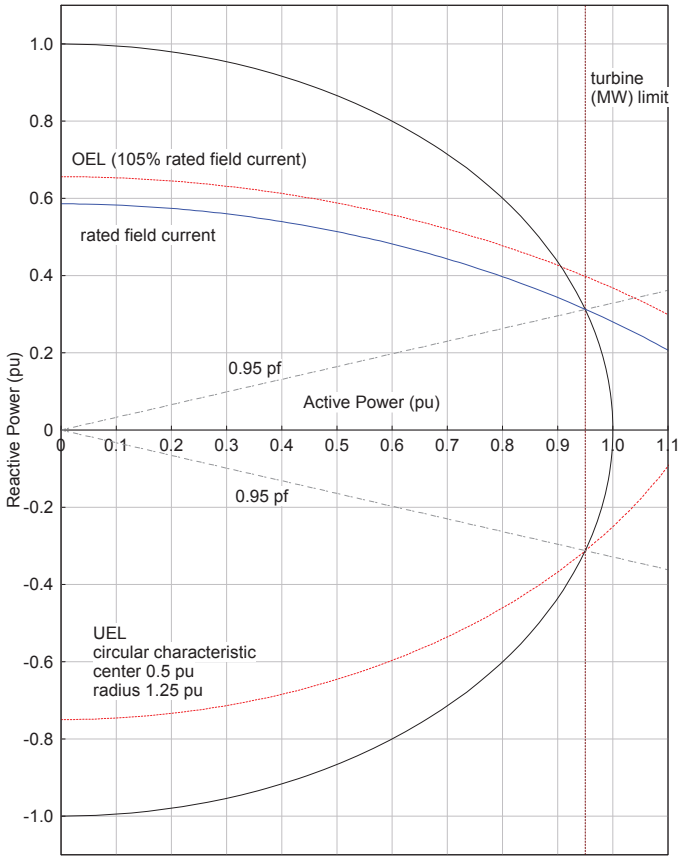

Figure 11: capability curves of salient-pole generators (identified in Table 12)

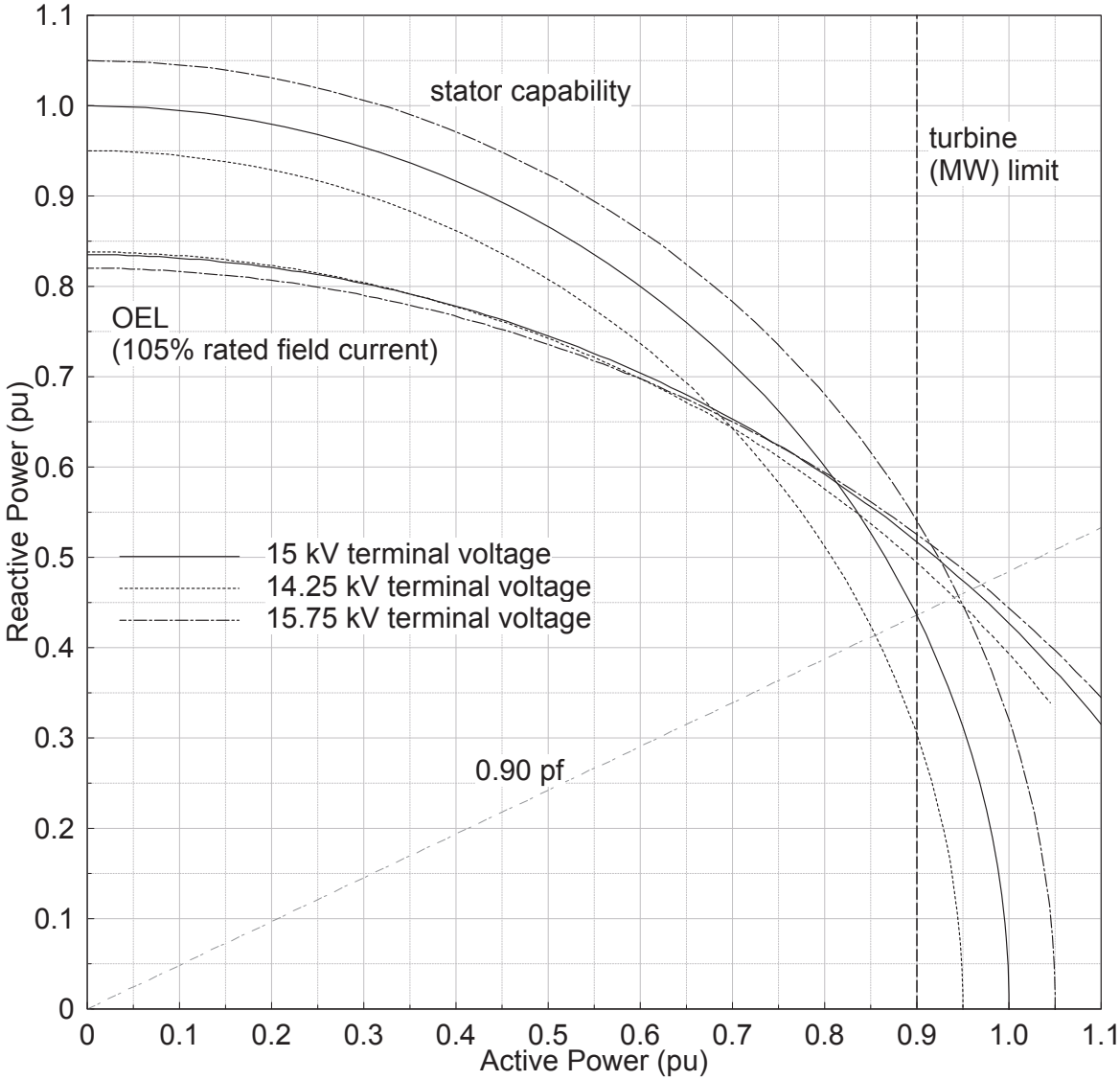

Figure 12: (partial) capability curves of round-rotor generators (identified in Table 12) for different terminal voltages

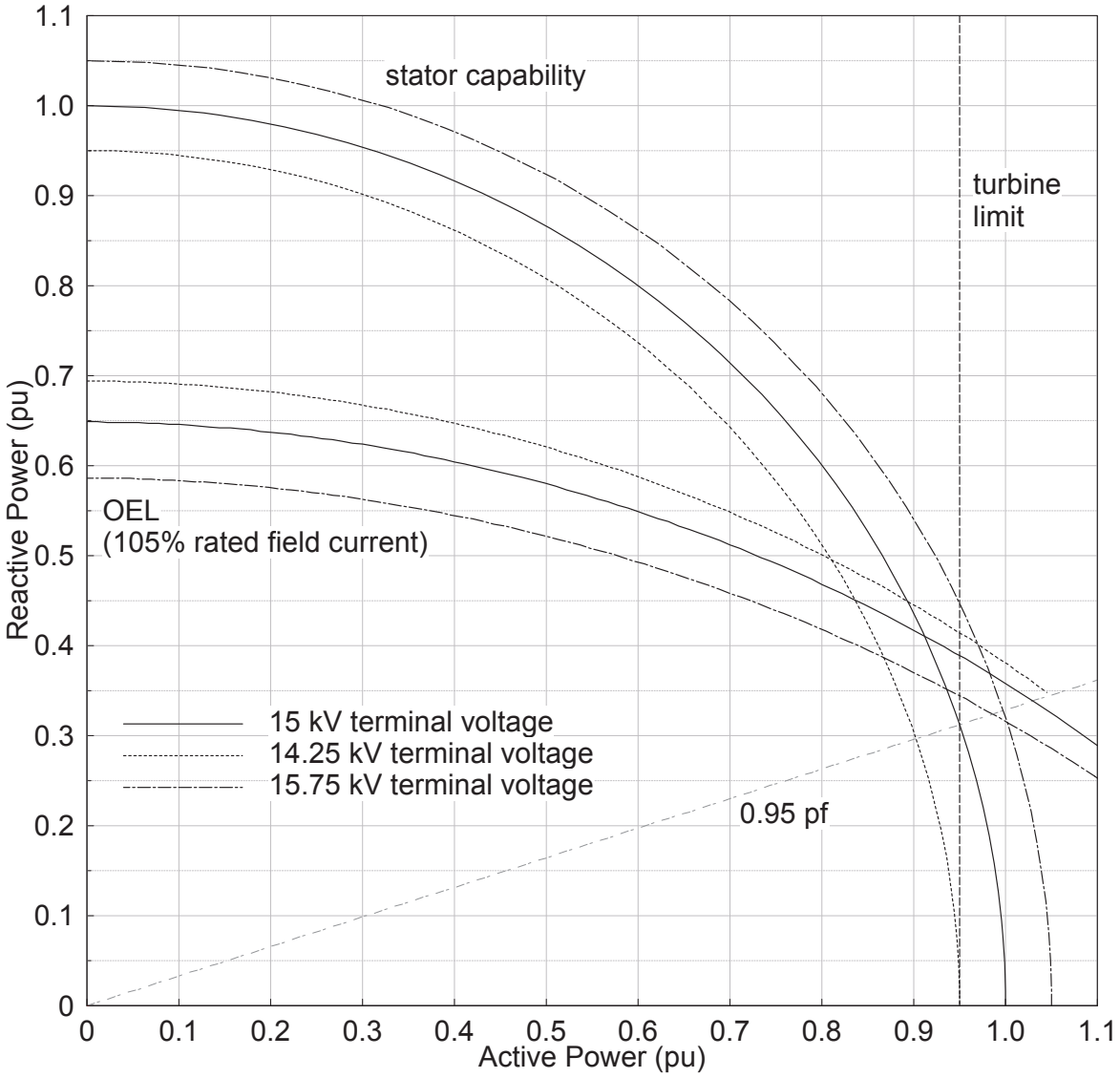

Figure 13: (partial) capability curves of salient-pole generators (identified in Table 12) for different terminal voltages

2.7 Turbine model and data

For already explained reasons, a constant mechanical torque is assumed for the machines of thermal plants. The hydraulic turbines have the nominal active power P_{nom} listed in Table 11. They are all represented by the simple, lossless model of Fig. 14 with a water time constant T_w of 1 second. In this model, z is the gate opening, q the water flow, H the head, P_m the mechanical power and T_m the mechanical torque, all in pu on the P_{nom} base. ω is the rotor speed in pu.

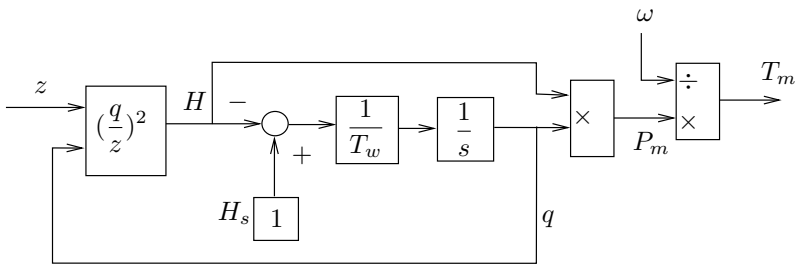

Figure 14: Model of hydro turbine

2.8 Speed governor model and data

The model of the speed governor used for all hydro turbines is shown in Fig. 15. The model includes a simple power measurement, a PI control and a servomotor. P is the active power produced by the generator, P^o is the power setpoint, z is the gate opening and ω is the rotor speed. All four are in per unit; for P and P^o the base is the turbine nominal power. The servomotor is represented by a first-order system with a time constant of 0.2 s, non-windup limits on z, and limits on the derivative of z. Only the value of the permanent speed droop σ varies from one machine to another, as indicated in Table 14.

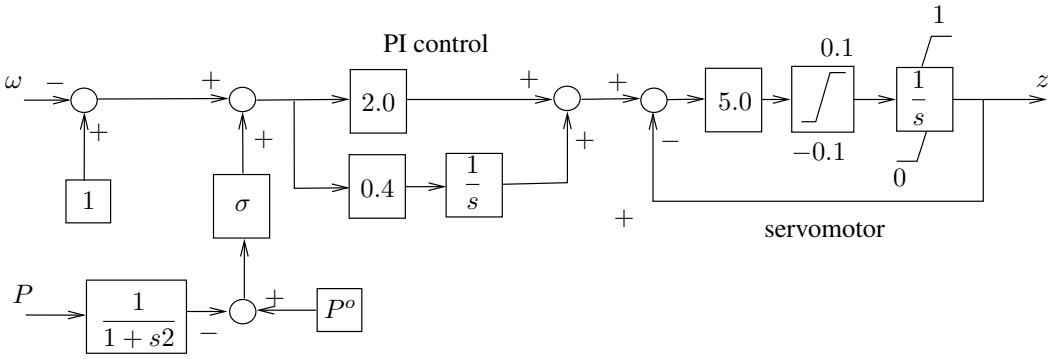

Figure 15: Model of speed governor

Table 14: Permanent speed droops of the speed governors

generators	σ
g19, g20	0.08
g1 - g5, g8 - g12	0.04

2.9 Load data

All loads are connected to the 20-kV buses. They have an exponential model:

$$P = P_o(\frac{V}{V_o})^{\alpha} \qquad Q = Q_o(\frac{V}{V_o})^{\beta} \tag{1}$$

with $\alpha = 1.0$ (constant current) and $\beta = 2.0$ (constant impendance), respectively. V_o is set to the initial voltage at the bus of concern.

2.10 Load tap changer data

All distribution transformers are equipped with LTCs keeping the distribution voltage in the deadband $[0.99\ 1.01]$ pu [4]. The LTCs adjust the transformer ratios in the range $[0.88\ 1.20]$ over 33 positions (thus from one position to the next, the ratio varies by 0.01).

The LTCs have intentional delays. When the distribution voltage leaves the above deadband at time t_o, the first tap change takes place at time $t_o + \tau_1$ and the subsequent changes at times $t_o + \tau_1 + k\tau_2$ $(k = 1, 2, \ldots)$. The delay is reset to τ_1 after the controlled voltage has re-entered (or jumped from one side to the other of) the deadband. The values of τ_1 and τ_2 are given in Table 15; they differ from one transformer to another in order to avoid unrealistic tap synchronization.

3 Dynamic responses to contingencies

3.1 Operating point A

The system response to a particular disturbance is considered. The system initially operates at point A, detailed in Section 2.2.1.

3.1.1 Disturbance

The disturbance of concern is a three-phase solid fault on line 4032-4044, near bus 4032, lasting 5 cycles (0.1 s) and cleared by opening the line, which remains opened.

The initiating fault is simulated to be more realistic but it is the resulting line outage that causes long-term voltage instability. Simulating the line outage without the fault would yield similar results, with some discrete events shifted in time.

[4] It can be checked in Table 10 that all initial bus voltages lie in this deadband

Table 15: Delays of load tap changers

transformer	delays	
	τ_1 (s)	τ_2 (s)
11-1011	30	8
12-1012	30	9
13-1013	30	10
22-1022	30	11
1-1041	29	12
2-1042	29	8
3-1043	29	9
4-1044	29	10
5-1045	29	11
31-2031	29	12
32-2032	31	8
41-4041	31	9
42-4042	31	10
43-4043	31	11
46-4046	31	12
47-4047	30	8
51-4051	30	9
61-4061	30	10
62-4062	30	11
63-4063	30	12
71-4071	31	9
72-4072	31	11

3.1.2 Voltages

The evolution of transmission system voltages is shown in Fig. 16.

In response to the initial disturbance, the system undergoes electromechanical oscillations that die out in 20 seconds. Then, the system settles at a short-term equilibrium, until the LTCs start acting at $t = 35$ s. Subsequently, the voltages evolve under the effect of LTCs and OELs.

The system is long-term voltage unstable and eventually collapses less than 3 minutes after the initiating line outage.

As illustrated by the figure, essentially the Central area is affected; voltages at Northern or Southern buses are comparatively little influenced.

3.1.3 Generator field currents and terminal voltages

Figures 17 and 18 show the evolution of field currents. After settling to post-disturbance values, they start increasing at $t = 35$ s, when the LTCs start acting. Figure 17 refers to the seven generators that get limited: these are in order g12, g14, g7, g11, g6, g15 and g16. Figure 18 refers to three non limited generators.

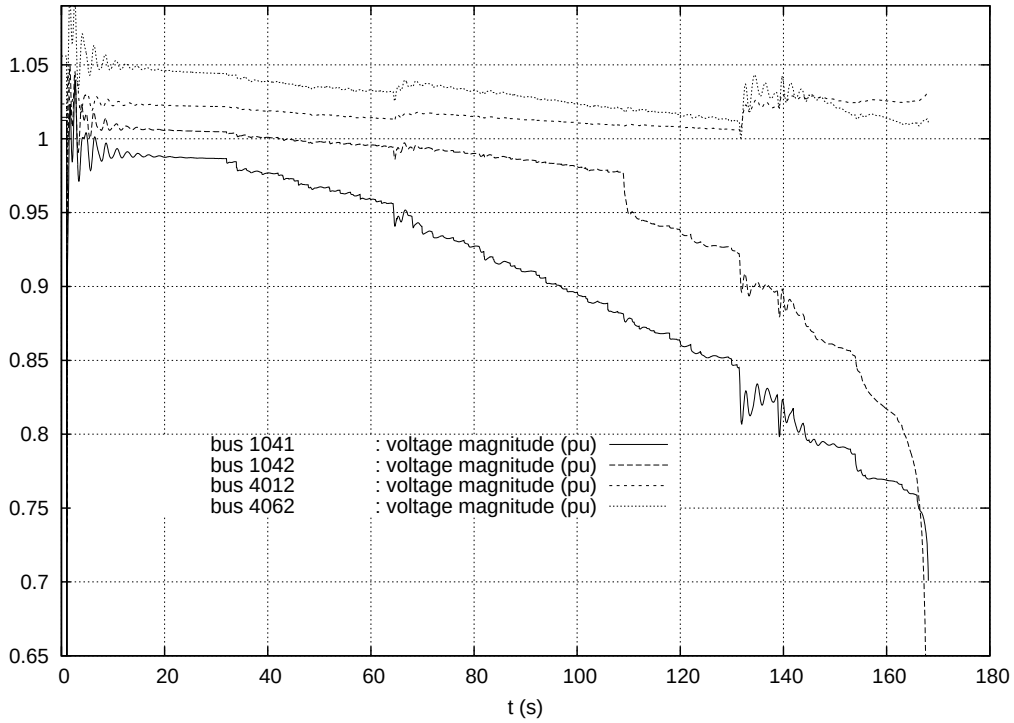

Figure 16: operating point A, fault on line 4032-4044 cleared by opening line: transmission voltages

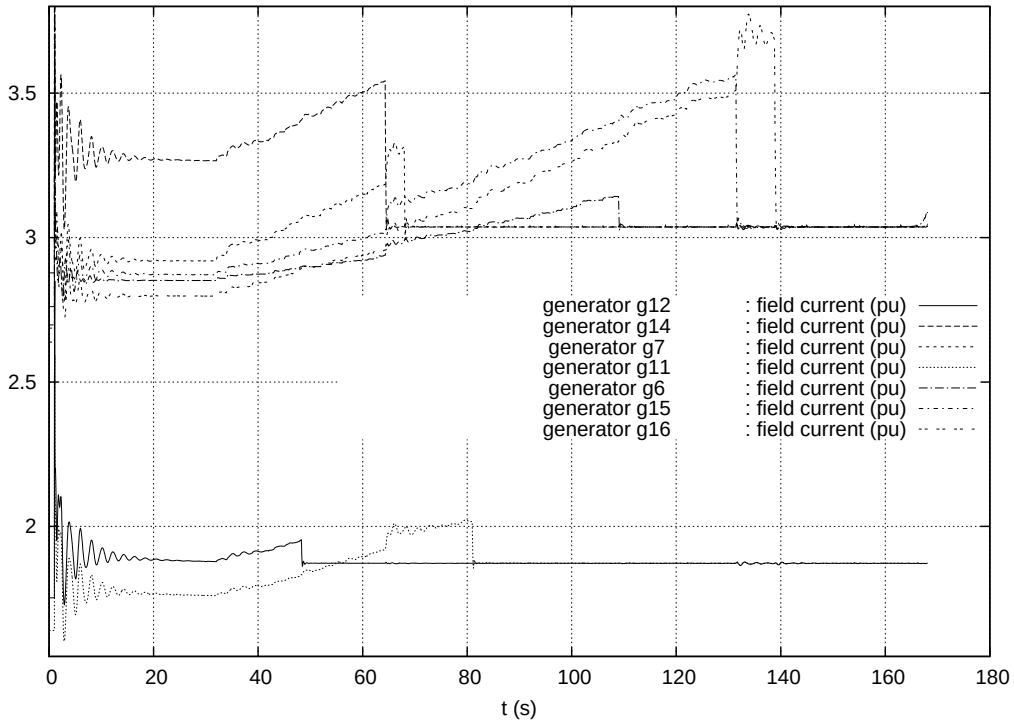

Figure 17: operating point A, fault on line 4032-4044 cleared by opening line: field currents of the seven limited generators

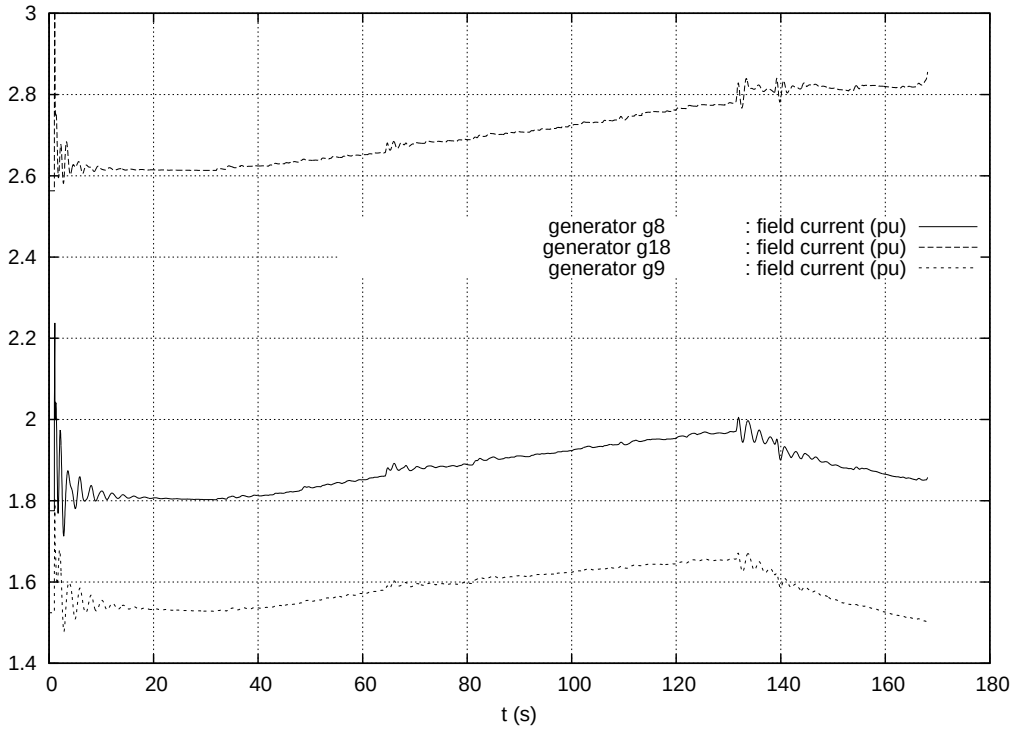

Figure 18: operating point A, fault on line 4032-4044 cleared by opening line: field currents of three non limited generators

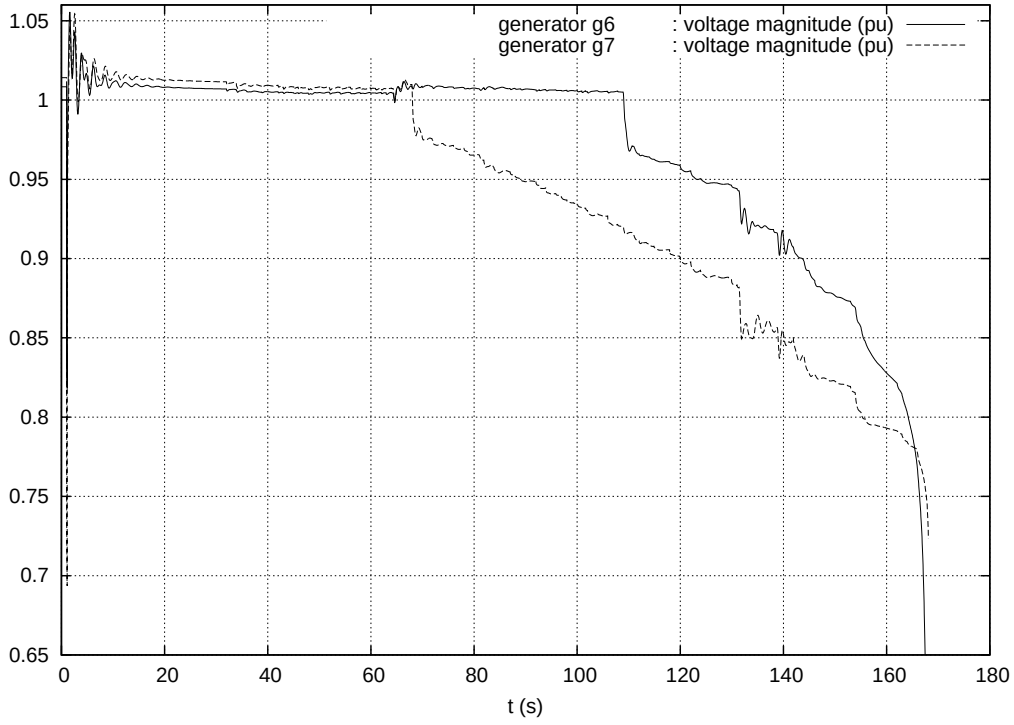

Figure 19: operating point A, fault on line 4032-4044 cleared by opening line: terminal voltages of two generators that get limited

Figure 19 shows the terminal voltages of two limited generators. It is easily seen that the voltage is kept fairly constant by the automatic voltage regulator, until the field current gets limited. After that, the voltage drops are pronounced. Note that the voltage of generator g7 eventually reaches a very low value. In a more realistic simulation, this generator should be tripped under the effect of an undervoltage protection, which would obviously aggravate the system degradation. For instance, assuming that this protection is set to act at a generator voltage of 0.85 pu, the tripping would take place near $t = 140$ s. It is acceptable to ignore the presence of such an undervoltage protection since, at $t = 140$ s, the system operating conditions are already unacceptable and other models, in particular that of loads, should be also adjusted.

3.1.4 Transformer ratios

Figure 20 shows a sample of distribution transformer ratios evolving with various delays to control distribution voltages.

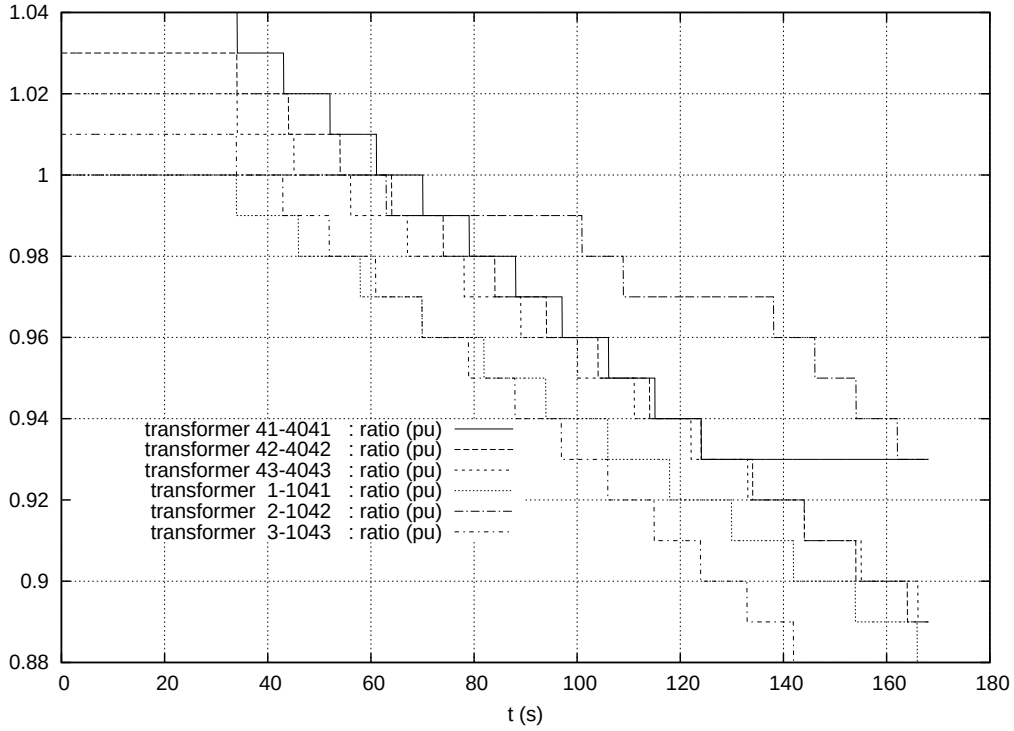

Figure 20: operating point A, fault on line 4032-4044 cleared by opening line: distribution transformer ratios

A more detailed view is given in Fig. 21, which refers to the transformer connected at bus 1041 and feeding the distribution bus 1. The plot shows the unsuccessful attempt to bring the distribution voltage of bus 1 back within the $[0.99\ 1.01]$ pu deadband.

The figure also illustrates the multi-dimensional aspect of the problem, i.e. interactions between the various LTCs. Indeed, it is seen that each tap change makes the corresponding distribution voltage move towards the target deadband but in between tap changes, the same voltage drops under the effect of the other LTCs acting

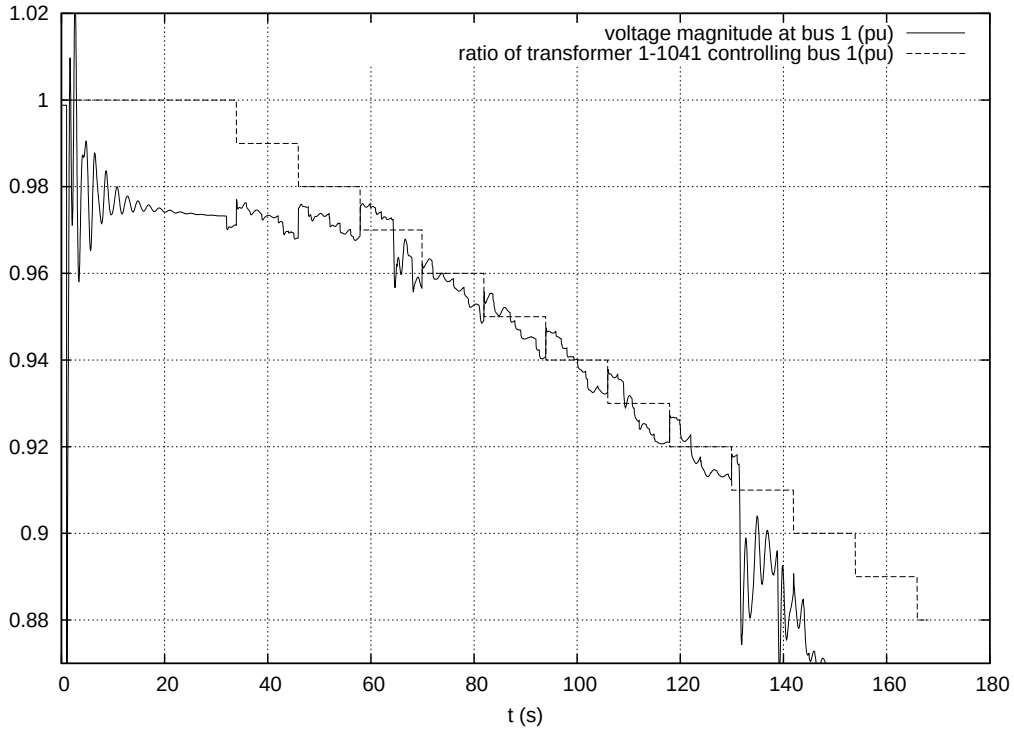

Figure 21: operating point A, fault on line 4032-4044 cleared by opening line: unsuccessful restoration of a distribution voltage by LTC

to restore their own voltages [5]. All in all, the distribution voltages, and hence the load powers cannot be restored, which is typical of long-term voltage instability.

3.1.5 Rotor speeds and angles

Fig. 22 shows the rotor speed deviations of respectively g6, g7 (both located in Central area), g17 (located in the South) and g20 (large equivalent generator in the North). The machines swing with respect to each other in a stable way until $t \simeq 170$ s, when g6 eventually separates from the other generators.

The curves also show the frequency deviations in response to the variations of load active power with voltages. The jumps at $t \simeq 65$ and 132 s correspond to machines switching under field current limit, which causes voltages, and hence load powers, to drop.

The final loss of synchronism of g6 with respect to the other machines, which causes the final system collapse, is confirmed by Fig. 23 showing the deviations of rotor angles with respect to the Center Of Inertia (COI) of the system.

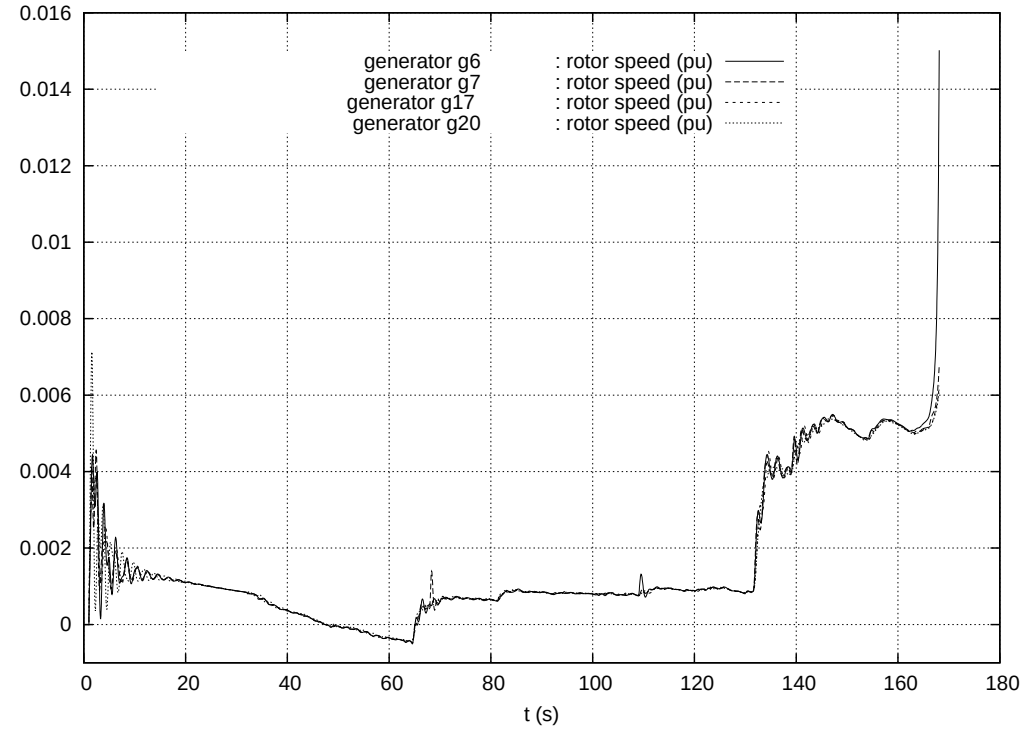

Figure 22: operating point A, fault on line 4032-4044 cleared by opening line: speed deviations of synchronous machines

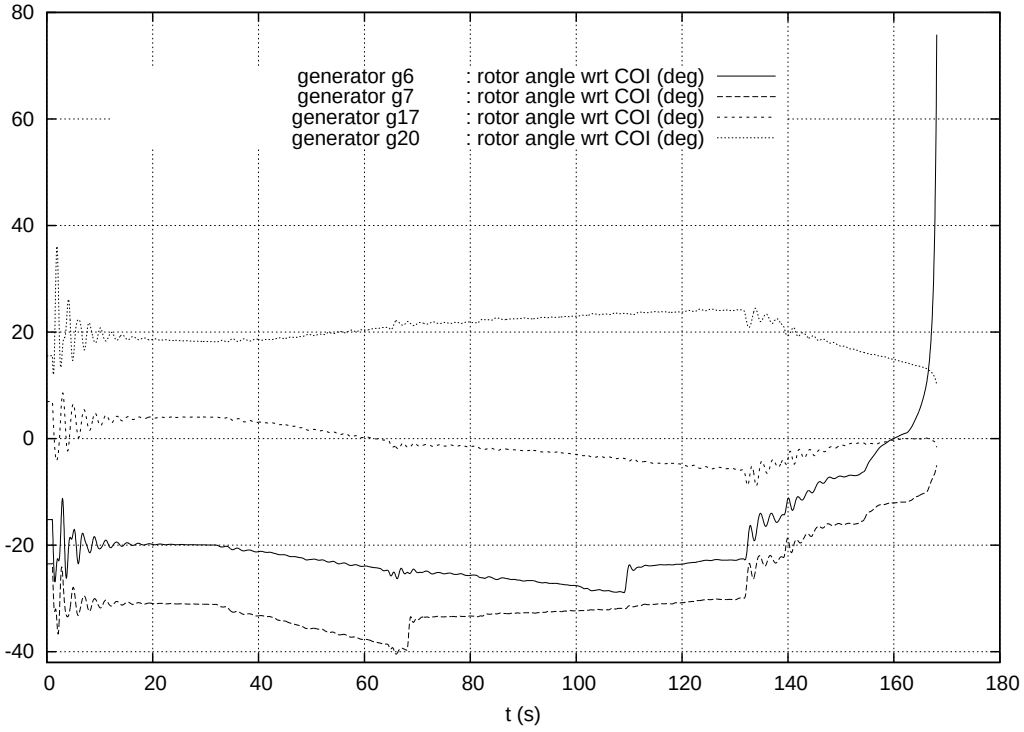

Figure 23: operating point A, fault on line 4032-4044 cleared by opening line: deviations of rotor angles of synchronous machines with respect to the Center Of Inertia (COI)

3.2 Operating point B

At this operating point, an exhaustive contingency analysis has been performed using time simulation.

The following contingencies have been considered:

- a 5-cycle (0.1 s) fault on any line, cleared by tripping the line;
- the outage of any single generator, except g19 and g20, which are equivalent generators. This includes the outage of one among the generators: g15, g15b, g16, g16b, g18 and g18b[5].

The post-contingency evolution has been considered acceptable if, over a simulation interval of 600 seconds:

- all distribution bus voltages are restored in their $[0.99\ 1.01]$ pu deadbands;
- no generator has its terminal voltage falling below 0.85 pu, except possibly for the fault-on period;
- no loss of synchronism takes place.

By way of illustration, Fig. 24 shows the stable evolution of the voltage at bus 1041 for the previously considered disturbance, namely a fault on line 4032-4044, cleared by opening the line. Fig. 25, relative to the same disturbance, shows five distribution voltages that are successfully restored in their deadbands by LTCs.

With the exception of one disturbance, all system responses satisfy the above criteria.

The exception is the outage of generator g6. The evolutions of voltages at the 130-kV buses of the Central region are shown in Fig. 26. It is clear that the impact is limited to bus 1042. The corresponding distribution voltages are shown in Fig. 27. It can be seen that the LTCs succeed restoring the distribution voltages in their deadbands, except the one controlling bus 2. After a number of unsuccessful steps, the ratio of transformer 1042-2 hits its lower limit, which explains the pseudo-stabilization of the system, though with unacceptably low voltages at buses 1042 and 2.

This very localized problem could be easily solved by providing bus 1042 with shunt compensation switched upon detection of a low voltage[6]. For instance, Fig. 28 shows the voltages at the above two buses when two shunt capacitors, each of 80 Mvar nominal power, respectively 10 and 20 seconds after the disturbance occurrence. The transmission voltage recovers to an acceptable value, while the LTC succeeds restoring the distribution voltage.

In view of the very localized nature of the problem, and the ability to solve it through corrective, post-disturbance control, it is reasonable to consider operating point B as secure.

[5] let us recall that the nominal powers of g15, g15b, g18 and g18b have been halved compared to operating point A

[6] bus 1042 is the only 130-kV bus not provided with shunt compensation

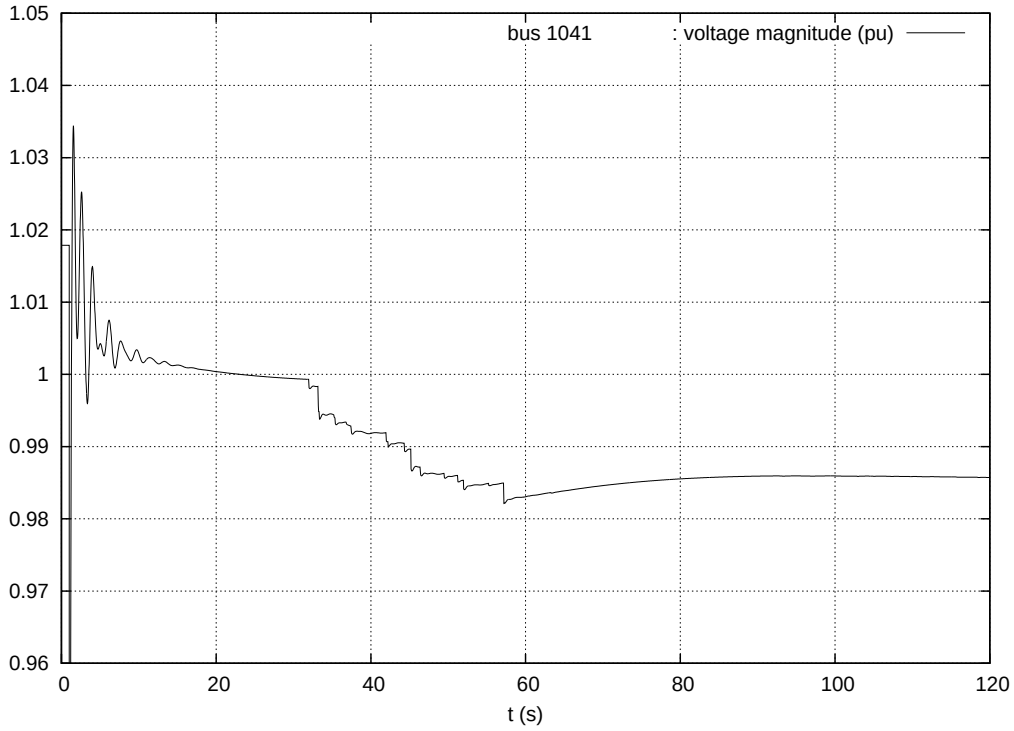

Figure 24: operating point B, fault on line 4032-4044 cleared by opening line: transmission voltages

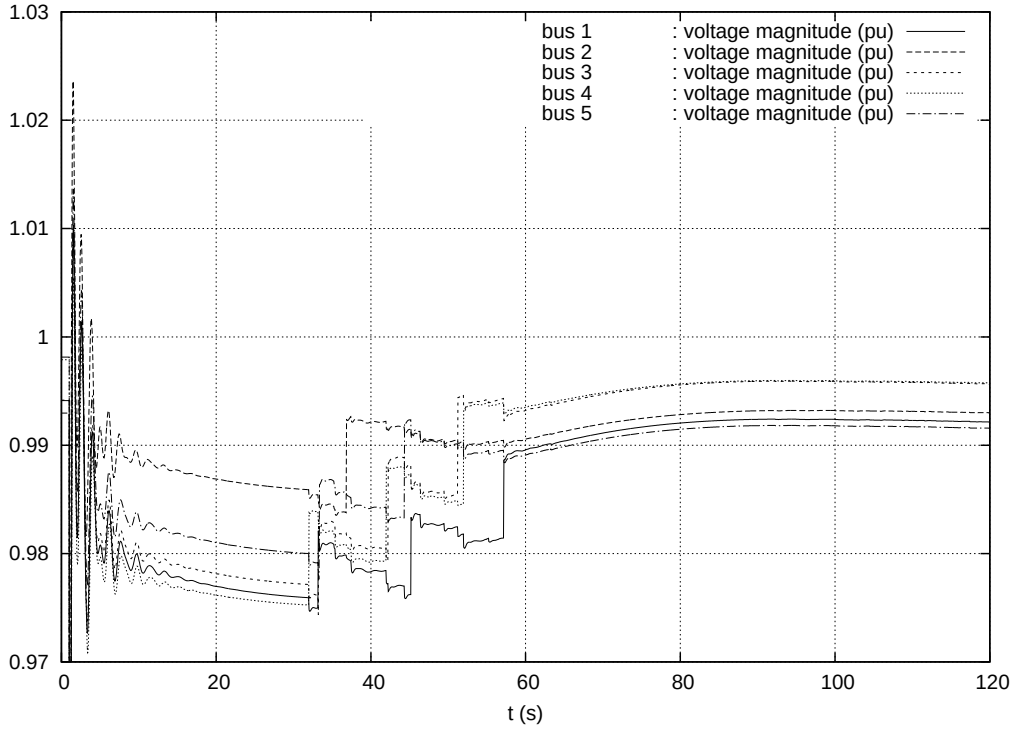

Figure 25: operating point B, fault on line 4032-4044 cleared by opening line: distribution voltages

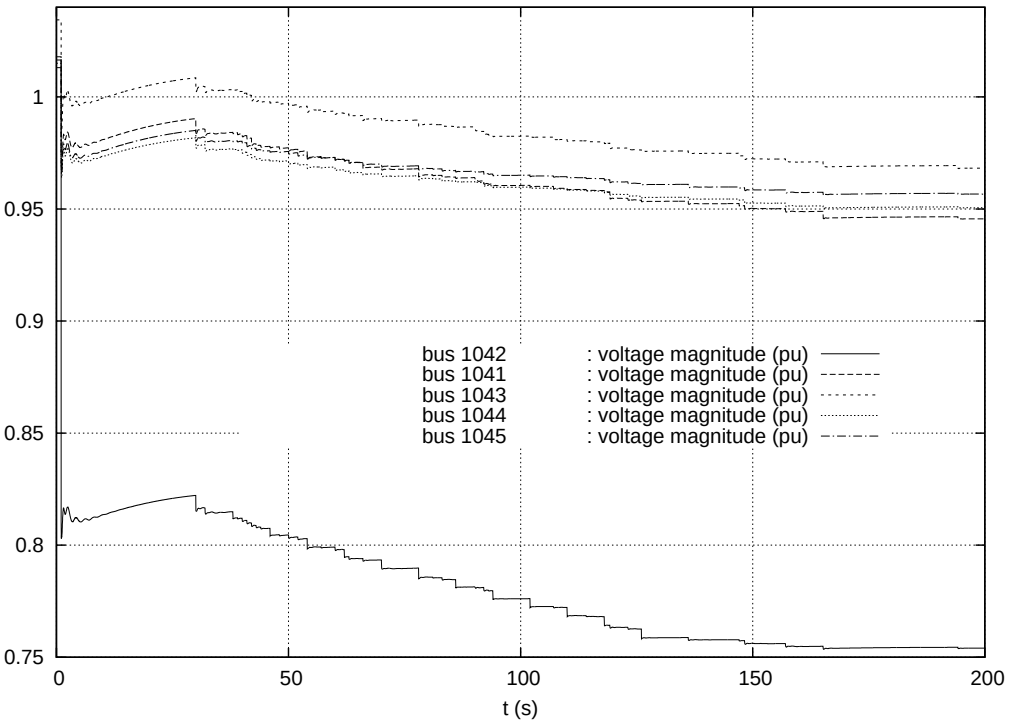

Figure 26: operating point B, outage of generator g6: transmission voltages

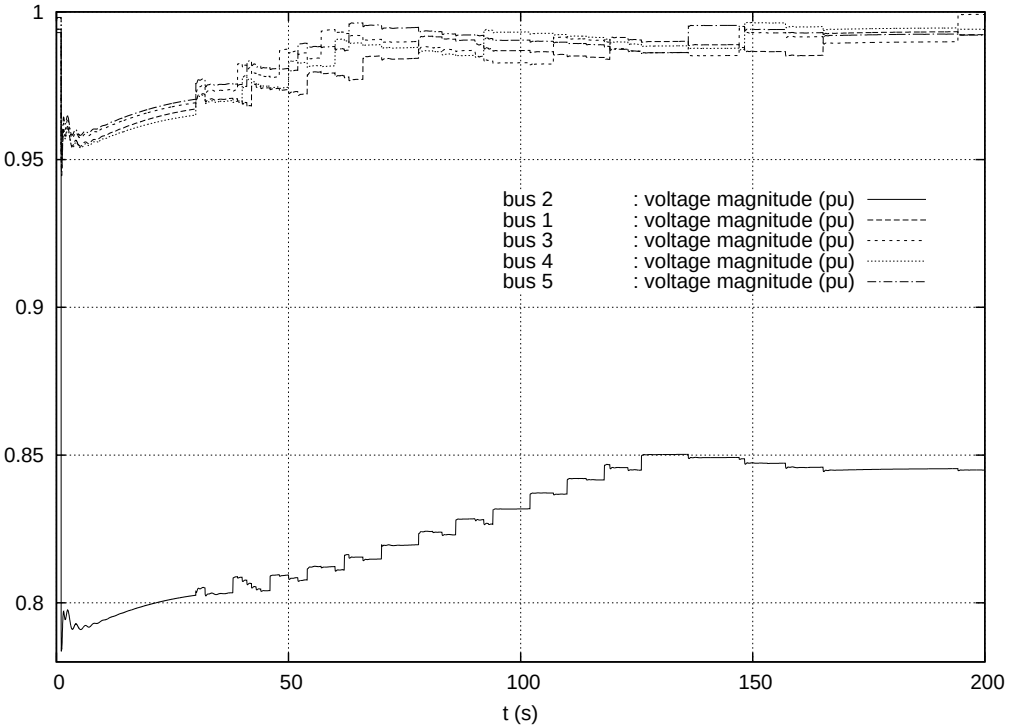

Figure 27: operating point B, outage of generator g6: distribution voltages

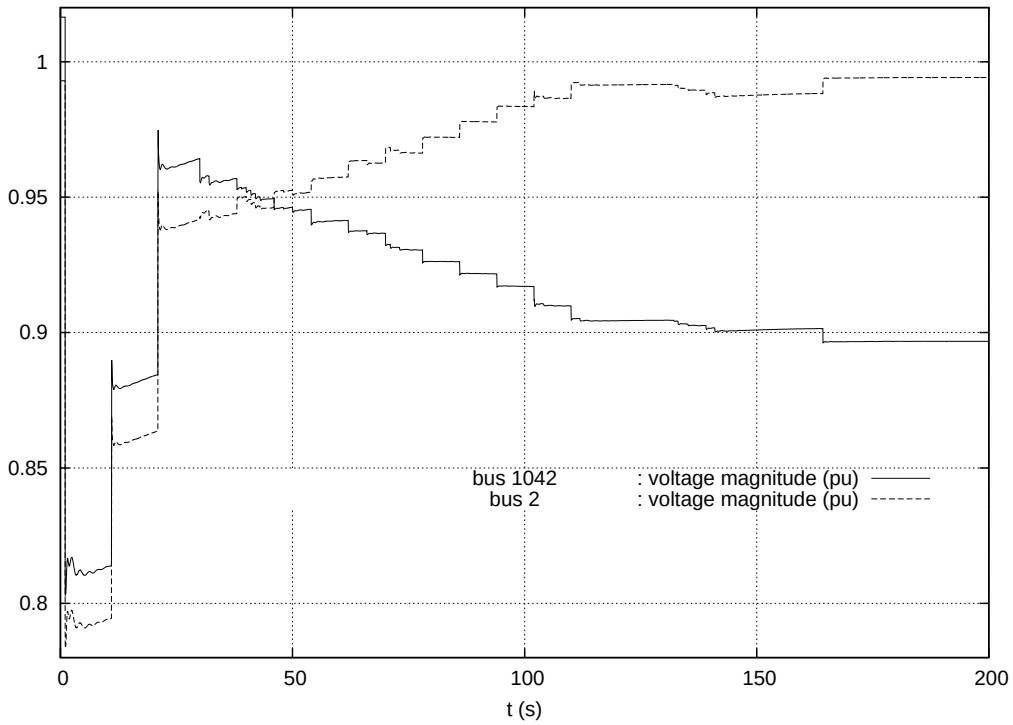

Figure 28: operating point B, outage of generator g6 followed by shunt compensation switching: transmission and distribution voltages

4 Examples of preventive security margin computations

This section is devoted to the determination of Secure Operation Limits (SOL) and power margins for the system operating at point B.

4.1 Secure operation limit: definition

An SOL involves stressing the system in its pre-contingency configuration. The stress considered here is an increase of loads in the Central area.

The SOL corresponds to the maximum load power that can be accepted in the pre-contingency configuration such that the system responds in a stable way to each of the specified contingencies [4].

To this purpose, power flow computations are performed for increasing values of the Central active and reactive loads. For each so determined operating point, the disturbance is simulated and the system response is analyzed.

In all cases, the criteria that lead to accepting the system response are those detailed in Section 3.2.

4.2 Pre-contingency stress

The Central area load is increased by steps of 25 MW. The total active power variation is shared by the 11 loads present in this area, in proportion to their base case value. The power factor of each load is kept constant. The active power variations are compensated by generator g20, taken as slack-bus.

In the pre-contingency power flow calculations, transformer ratios are adjusted in response to load changes as follows:

1. the 22 distribution transformers are adjusted in order to maintain the distribution voltages in the dead-bands as previously described;
2. the 400/130-kV transformers 1044-4044, 1044-4044b, 1045-4045 and 1045-4045b are assumed to be controlled by operators, adjusting their ratio to maintain the voltages at buses 1044 and 1045 in deadbands. Note that these transformers do not have their tap changed in the post-disturbance simulation, whose duration is considered too short for operators to react.

In both cases, ratios are modified when the controlled voltages leave their deadbands, and vary in discrete steps. The ratios of transformers in parallel are varied together.

The data of the distribution transformers have been given in Section 2.10, while Table 16 gives the data relative to the 400/130 kV transformers.

Table 16: Data for pre-contingency adjustment of the 400/130-kV transformers

transformer	controlled bus	minimum ratio	maximum ratio	number of tap positions	voltage deadband (pu)
1044-4044	1044	0.87	1.11	25	[1.0006 1.0206]
1044-4044b	1044	0.87	1.11	25	[1.0006 1.0206]
1045-4045	1045	0.87	1.11	25	[1.0046 1.0246]
1045-4045b	1045	0.87	1.11	25	[1.0046 1.0246]

Table 17 provides the values of the transformer ratios for various pre-contingency load levels mentioned in this section.

Table 17: Pre-contingency transformer ratios

transformer	base case ratio	ratio after a load increase (in MW) of								
		25	50	100	250	275	350	375	400	500
1044-4044	1.08	1.08	1.08	1.08	1.06	1.06	1.05	1.05	1.05	1.03
1044-4044-2	1.08	1.08	1.08	1.08	1.06	1.06	1.05	1.05	1.05	1.03
1045-4045	1.09	1.09	1.09	1.08	1.07	1.07	1.06	1.06	1.05	1.04
1045-4045-2	1.09	1.09	1.09	1.08	1.07	1.07	1.06	1.06	1.05	1.04
11-1011	1.06	1.06	1.06	1.06	1.06	1.06	1.06	1.06	1.06	1.05
12-1012	1.06	1.06	1.06	1.06	1.06	1.06	1.06	1.06	1.06	1.06
13-1013	1.04	1.04	1.04	1.04	1.04	1.04	1.04	1.04	1.04	1.04
22-1022	1.08	1.08	1.08	1.08	1.07	1.07	1.07	1.06	1.06	1.05
1-1041	1.01	1.01	1.00	1.00	0.99	0.99	0.98	0.98	0.98	0.98
2-1042	1.01	1.01	1.01	1.00	1.00	1.00	1.00	0.99	0.99	0.99
3-1043	1.02	1.02	1.01	1.01	1.00	1.00	1.00	0.99	0.99	0.99
4-1044	1.00	1.00	1.00	0.99	0.99	0.99	0.99	0.98	0.98	0.98
5-1045	1.00	1.00	1.00	1.00	0.99	0.99	0.99	0.99	0.99	0.99
31-2031	1.07	1.07	1.07	1.07	1.06	1.05	1.05	1.04	1.04	1.03
32-2032	1.07	1.07	1.07	1.07	1.07	1.07	1.07	1.07	1.07	1.06
41-4041	1.09	1.09	1.09	1.09	1.08	1.07	1.07	1.06	1.06	1.05
42-4042	1.08	1.08	1.08	1.08	1.06	1.06	1.05	1.05	1.04	1.03
43-4043	1.07	1.07	1.07	1.07	1.05	1.05	1.04	1.04	1.04	1.02
46-4046	1.06	1.06	1.06	1.06	1.05	1.04	1.04	1.03	1.03	1.02
47-4047	1.06	1.06	1.06	1.06	1.05	1.05	1.05	1.04	1.04	1.03
51-4051	1.08	1.08	1.08	1.08	1.08	1.07	1.07	1.07	1.07	1.06
61-4061	1.05	1.05	1.05	1.05	1.05	1.05	1.04	1.04	1.04	1.03
62-4062	1.05	1.05	1.05	1.05	1.05	1.05	1.05	1.05	1.05	1.05
63-4063	1.03	1.03	1.03	1.03	1.03	1.03	1.03	1.03	1.03	1.03
71-4071	1.03	1.03	1.03	1.03	1.03	1.03	1.03	1.03	1.03	1.03
72-4072	1.05	1.05	1.05	1.05	1.05	1.05	1.05	1.05	1.05	1.05

4.3 SOL with respect to the contingency of Section 3.1.1

First, the contingency of Section 3.1.1 is considered.

Figure 29 shows the post-disturbance evolution of the voltage at bus 1041, for various pre-contingency load levels. The case with 375 MW loading seems stable but instability is revealed at $t \simeq 800$ s. Thus, for that contingency, the power margin with respect to the SOL is 350 MW.

Incidentally, the figure illustrates the well-known fact that, in marginal cases, it takes more time for the system to show its stability or instability.

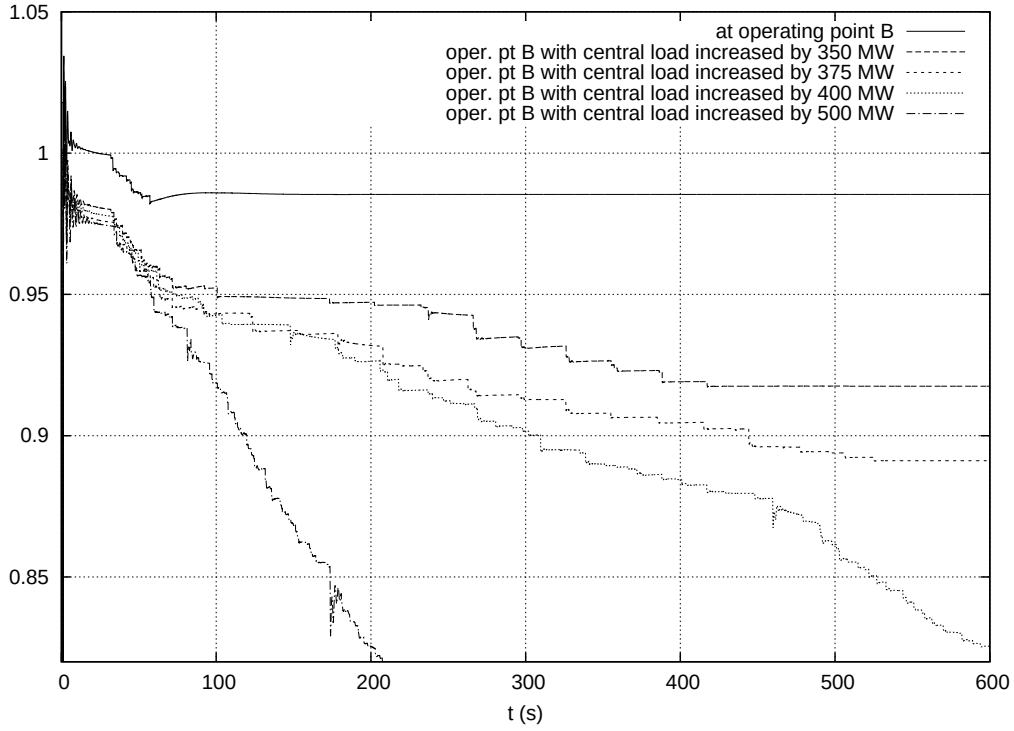

Figure 29: fault on line 4032-4044 cleared by opening line: evolution of voltage at bus 1041 for various pre-contingency stress levels

The SOL can be expressed in terms of the North-Central interface flow, which is the total power transfer across the North-Central border, shown with dotted line in Fig. 1, with the individual line flows measured at the Northern ends. The values are given at the bottom of Table **??**.

4.4 SOL with respect to generator outages

The contingencies of concern here are the outage (without fault) of any single generator, except g19 and g20, which are equivalents.

The outage of g14 is found the most severe with a power margin with respect to the SOL of only 25 MW !

Figure 30 shows the post-disturbance evolution of the voltage at bus 1041, for various pre-contingency load levels.

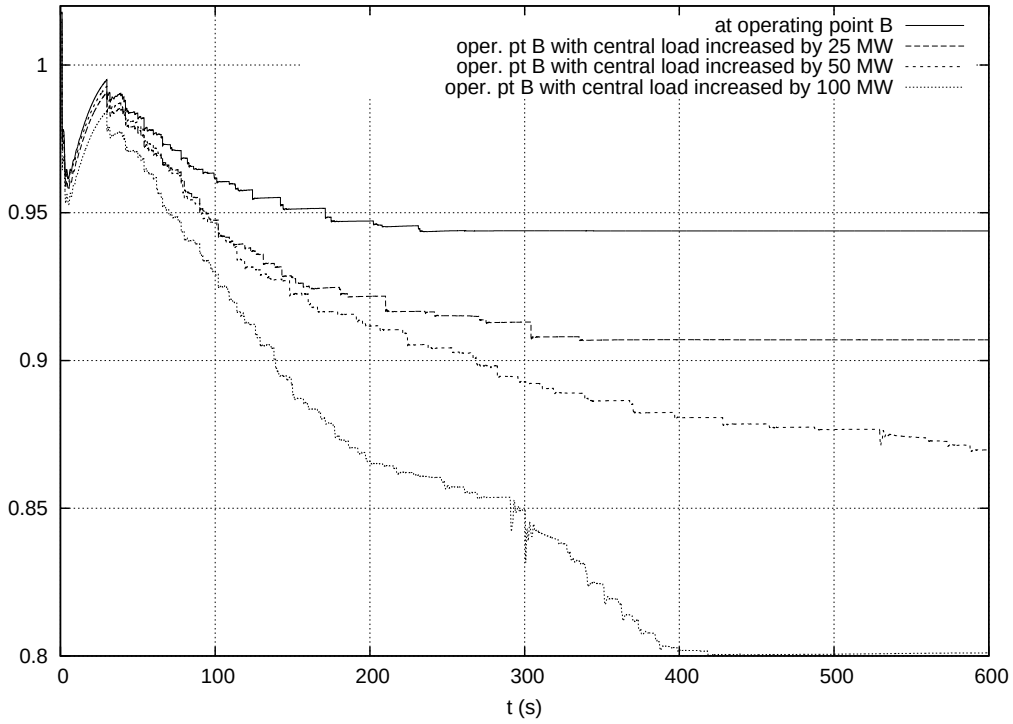

Figure 30: outage of generator g14: evolution of voltage at bus 1041 for various pre-contingency stress levels

The outage of g14 is a severe contingency because : (i) voltage control and reactive reserve are lost at bus g14, and (ii) the 630-MW power produced by g14 is compensated by the Northern and equivalent generators, which increases the North-Central power transfer.

4.5 SOL with respect to line outages

The contingencies of concern here are the tripping, after a 5-cycle fault, of any single transmission line[7].

The outage of line 4011-4021 is found the most severe with a power margin with respect to the SOL of 250 MW.

Figure 31 shows the post-disturbance evolution of the voltage at bus 4022, for various pre-contingency load levels.

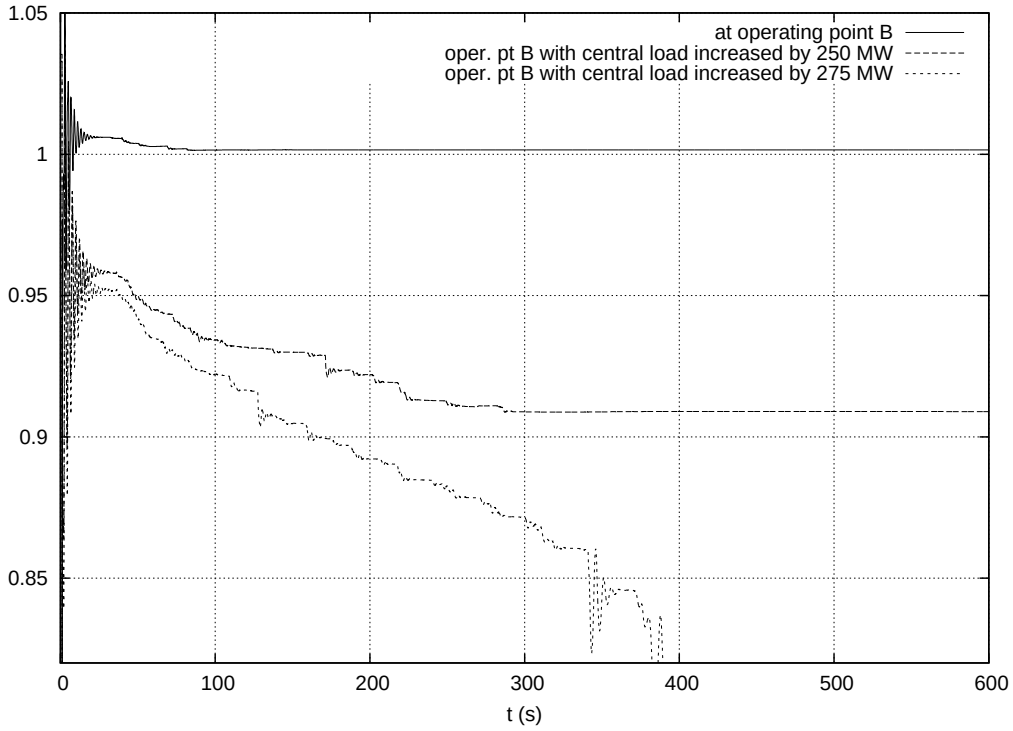

Figure 31: fault on line 4011-4021 cleared by opening line: evolution of voltage at bus 4022 for various pre-contingency stress levels

Note that this contingency involves a line located in the North area. The sequence of events is as follows. The outage of line 4011-4021 causes the active power to be redirected to the "corridor" between buses 4011, 4012, 4022 and 4031. This requires more reactive power support from generator g12. For a pre-contingency stress of 250 MW, g12 switches under field current limit at $t = 89$ s, while for a stress of 275 MW, this limitation takes place at $t = 67$ s. The earlier limitation confirms the higher reactive support by g12. As regards generator g8, for a stress of 250 MW, it remains under voltage control, while for a stress of 275 MW, it gets limited at $t = 340$ s. The switching of g8 under field current limit restarts some LTC actions, and the voltages keep on decreasing, until both generators, operating under constant excitation, lose synchronism by lack of synchronizing torque.

[7] transformers were not considered

5 Examples of corrective post-disturbance control

5.1 Modified tap changer control

This section and the next one illustrate emergency control actions, typical of System Integrity Protection Scheme (SIPS). Note that the material does not intend to be an exhaustive investigation of emergency controls; neither have these controls been "optimized" (for instance to minimize customer inconvenience).

The emergency control example consists of decreasing by 0.05 pu the voltage setpoint of LTCs controlling loads. This exploits the sensitivity of load power to voltage. For active power, with a constant current characteristic, one can expect a 5 % reduction, while for reactive power, with a constant impedance characteristic, one can expect a 10 % reduction.

Although many variants can be thought of, in the considered scenario the action is applied at $t = 100$ s, a little after the lowest transmission voltage (at bus 1041) has reached 0.90 pu. Two sets of LTCs have been considered:

- the five LTCs controlling loads at buses 1, 2, 3, 4 and 5;
- the same together with the six LTCs controlling loads at buses 41, 42, 43, 46, 47 and 51.

Figure 32 shows the evolution of the voltage magnitude at bus 1041 when reducing the setpoints of respectively the 5 LTCs and the 11 LTCs. For comparison purposes, it also shows the evolution without action on LTCs. It can be seen that acting on 5 LTCs is not sufficient: the system collapses a little later. On the other hand, acting on 11 LTCs is effective and even succeeds bringing the transmission voltage above its pre-disturbance value, although after a long time due to LTC delays.

Note that all generators that were switched under field current limit in the case without emergency control (see Fig. 17) now reset under voltage control after some time. Without their regaining voltage control, some severe overvoltages would be experienced in the transmission system.

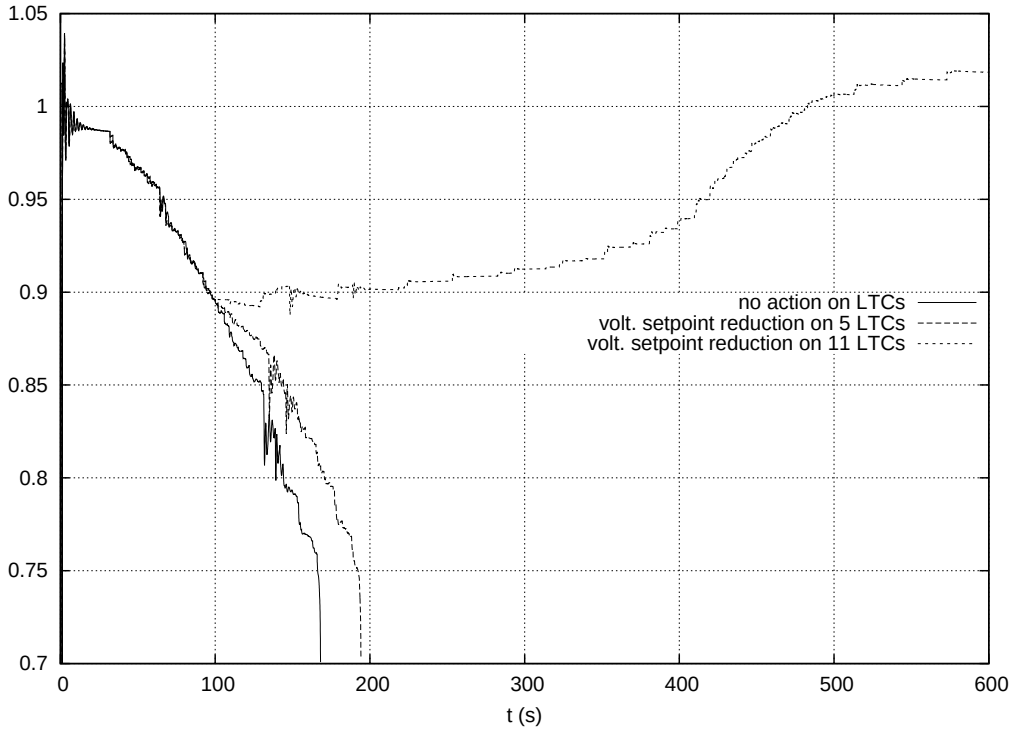

Figure 32: Evolution of voltage magnitude at bus 1041, without and with emergency control of LTCs

5.2 Undervoltage load shedding

The second example of emergency control deals with undervoltage load shedding. Distributed controllers have been considered as detailed in [7]. Each controller monitors the voltage at a transmission bus and acts on the load at the nearest distribution bus, according to the following simple logic:

> shed ΔP MW of load when the monitored voltage V goes below a threshold V^{th} for more than τ seconds.

Important features are the ability of each controller to act several times (a closed-loop behaviour that yields a robust and adaptive protection) and the absence of communication between controllers.

The example given hereafter has been obtained with $V^{th} = 0.90$ pu, $\Delta P = 50$ MW, and $\tau = 3$ seconds. Each time a block is shed, the value of P_o in (1) is decreased by ΔP and Q_o by ΔQ.ΔQ has been chosen so that the load power factor at 1 pu voltage is preserved.

Figure 33 shows the performance of the so adjusted load shedding controllers. Six blocks of load are shed, two by the controller monitoring bus 1041 and acting on bus 1 (at $t = 100$ and 144.95 s) and four by the controller of monitoring bus 1044 and acting on bus 4 (at $t = 112.10, 123.10$, 180.40 and 290.45 s), for a total of 300 MW.

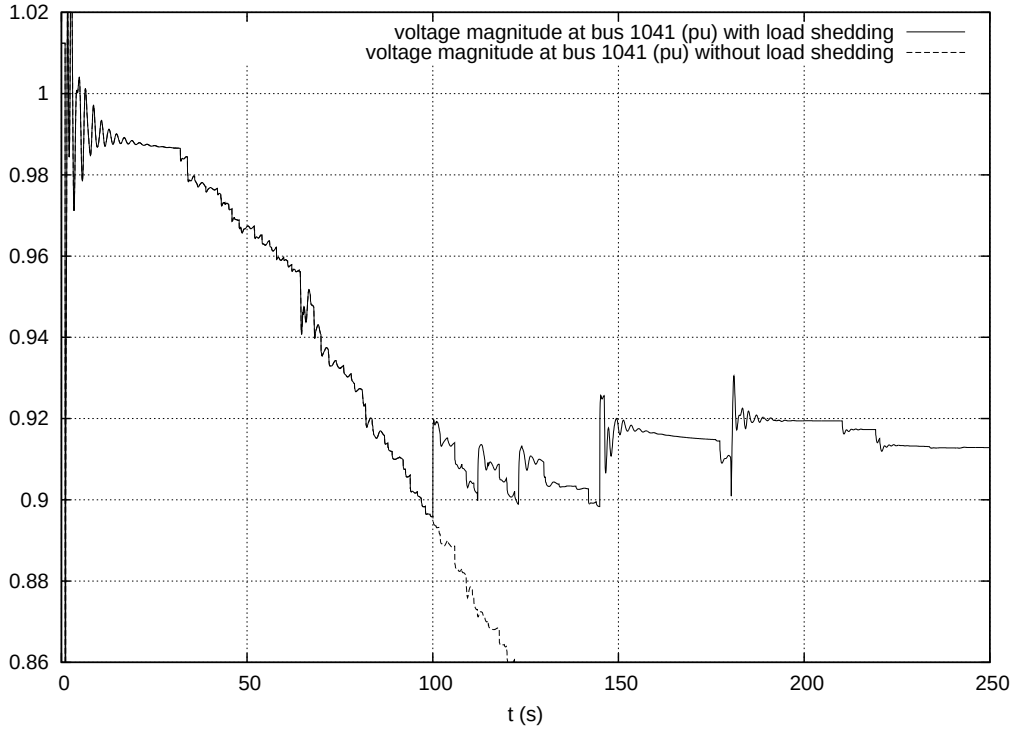

Figure 33: Evolution of voltage magnitude at bus 1041, without and with load shedding

Figure 34 shows the active powers of the loads at buses 1 and 4, respectively. The power evolves under the effect of LTCs and curtailments. The latter are easily identified from the curves. When one load is curtailed, its own power decreases while the other load power (slightly) increases, under the effect of the increasing voltage.

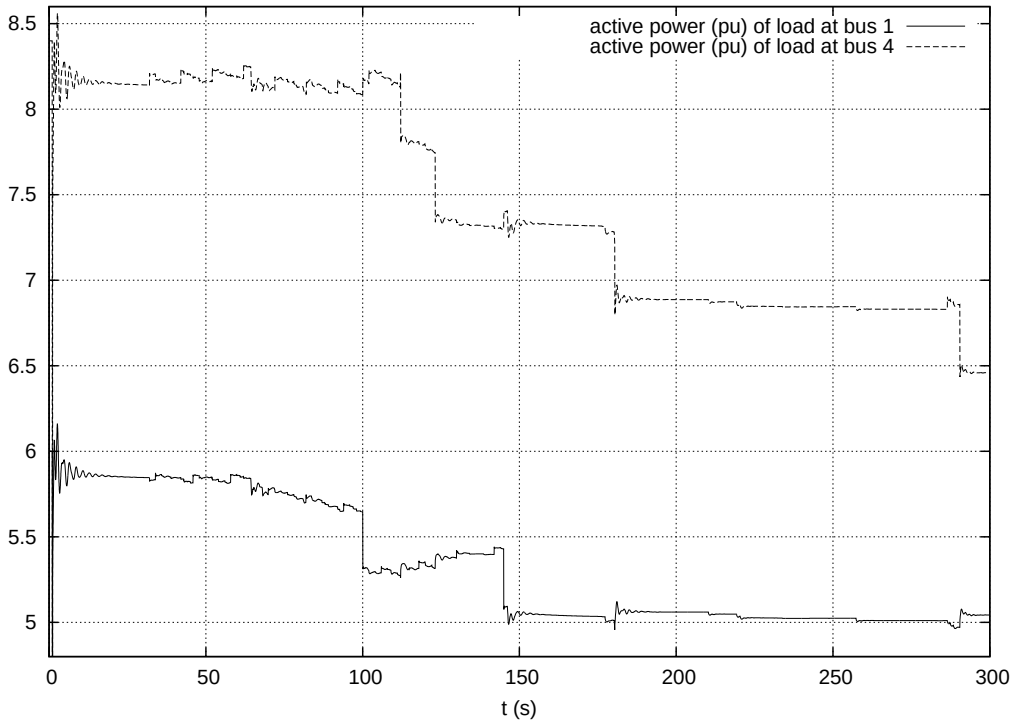

Figure 34: Evolution of active power of loads at buses 1 and 4, with load shedding

6 Long-term voltage instability analysis through sensitivities

Long-term voltage instability results from the attempt of loads to restore their powers at a level that the combined transmission and generation systems cannot provide [4]. In this test system, as in many real-life systems, load power restoration comes from the LTCs which try to restore load voltages. At the same time, the system weakening caused by the line outage reduces the maximum power that can be delivered to loads, while the reactive power limits of generators contribute to further reducing this power.

In their attempt to restore load power, the LTCs make the system pass through a maximum load power point. This is easily shown on the well-known 2-bus example: the system passes through the "nose" of the PV curve (determined with appropriate assumption on load reactive power). In a real-life system, it is a combination of load active and reactive powers that passes through a maximum. This can be detected with sensitivity analysis carried out along the system trajectory. We consider the sensitivity of the total reactive power generation to individual load reactive powers. When approaching the maximum power point, those sensitivities take larger and larger values while when crossing it, they suddenly change sign. More details can be found in [6], together with considerations on how synchronized phasor measurements could be used in the future to determine those sensitivities in a wide-area monitoring scheme.

The dashed line in Fig. 35 shows the sensitivity relative to bus 1041. The above mentioned sign change takes place at $t \simeq 87$ s. The corresponding point can be seen as lying on the nose of some PV curve. Figure 16 shows that voltages are still rather high at that point. The solid line in Fig. 35 is the same sensitivity computed with anticipation of generator limitation, i.e. as soon as a generator field current settles above the i_{fd}^{lim} limit, the OEL equation is anticipatively substituted to the AVR equation in the sensitivity calculation [6]. The figure shows that the resulting alarm takes place at $t \simeq 72$ s.

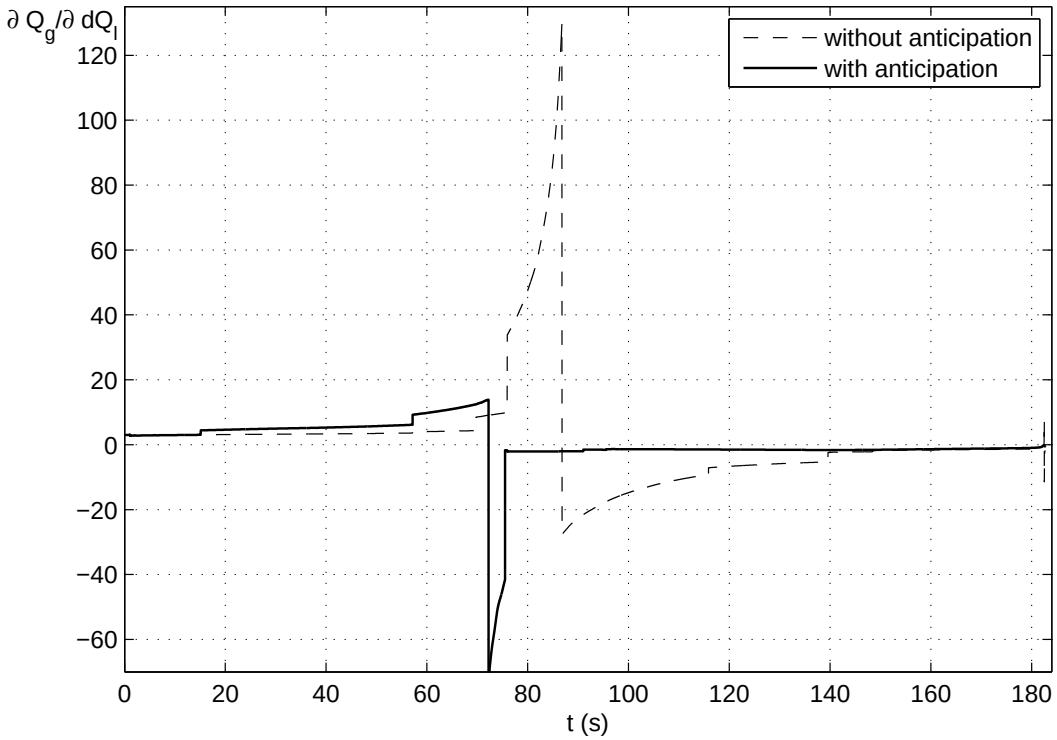

Figure 35: $\partial Q_g / \partial Q_l$ at bus 1041

References

[1] M. Stubbe (Convener), *Long-Term Dynamics - Phase II*, Report of CIGRE Task Force 38.02.08, Jan. 1995

[2] P. Kundur, *Power System Stability and Control*, Mc Graw Hill, EPRI Power System Engineering Series, 1994

[3] C. W. Taylor, *Power System Voltage Stability*, EPRI Power System Engineering Series, McGraw Hill, 1994

[4] T. Van Cutsem, C. Vournas, *Voltage stability of electric power systems*, Springer (previously Kluwer Academic Publishers), Boston (USA), 1998, ISBN 0-7923-8139-4

[5] C. Vournas, T. Van Cutsem, "Local Identification of Voltage Emergency Situations", IEEE Trans. on Power Systems, Vol. 23, No 3, 2008, pp. 1239-248. Available at http://ieeexplore.ieee.org (DOI 10.1109/TPWRS.2008.926425) and http://hdl.handle.net/2268/3194

[6] M. Glavic, T. Van Cutsem, "Wide-area Detection of Voltage Instability from Synchronized Phasor Measurements. Part I: Principle. Part II: Simulation Results", IEEE Trans. on Power Systems, Vol. 24, 2009, pp. 1408-1425. Available at http://ieeexplore.ieee.org (DOI 10.1109/TPWRS.2009.2023272) and http://hdl.handle.net/2268/7885

[7] B. Otomega, T. Van Cutsem, “Undervoltage load shedding using distributed controllers”, IEEE Trans. on Power Systems, Vol. 22, No 4, 2007, pp. 1898-1907. Available at http://ieeexplore.ieee.org (DOI 10.1109/TPWRS.2007.907354) and http://hdl.handle.net/2268/3050